UNIVERSIDADE ESTADUAL DE CAMPINAS
UNIVERSITY OF CAMPINAS

FACULDADE DE ENGENHARIA ELÉTRICA E DA COMPUTAÇÃO
SCHOOL OF ELECTRICAL AND COMPUTER ENGINEERING

ARAVIND KRISHNAN

Caracterização dos parâmetros de desvanecimento da distribuição alfa- mu: medidas e estatísticas

On the Fading Parameters Characterization of the alpha-mu distribution: Measurements and Statistics

Dissertação de Mestrado apresentada ao Programa de Pós-Graduação em Engenharia Elétrica da Faculdade de Engenharia Elétrica e de Computação da Universidade Estadual de Campinas para obtenção do título de Mestre em Engenharia Elétrica, na área de Telecomunicações.

Masters dissertation presented to the School of Electrical and Computer Engineering as a part of the requirement for obtaining M.Sc in Electrical Engineering in the field Telecommunications.

Orientador: Prof. Dr. Michel Daoud Yacoub
Co-Orientador: Prof. Dr. Ugo Silva Dias

Supervisor: Prof. Dr. Michel Daoud Yacoub
Co-Supervisor: Prof. Dr. Ugo Silva Dias

Campinas, Sao Paulo, Brazil
2011

FICHA CATALOGRÁFICA ELABORADA PELA
BIBLIOTECA DA ÁREA DE ENGENHARIA E ARQUITETURA - BAE - UNICAMP

K898f	Krishnan, Aravind On the fading parameters characterization of the alpha-mu distribution: measurements and statistics / Aravind Krishnan. --Campinas, SP: [s.n.], 2011. Orientador: Michel Daoud Yacoub Coorientador: Ugo Silva Dias. Dissertação de Mestrado - Universidade Estadual de Campinas, Faculdade de Engenharia Elétrica e de Computação. 1. Sistema de computação sem fio. 2. Radio - Transmissores e transmissão - Desvanecimentp. 3. Comunicação digital. I. Yacoub, Michel Daoud. II. Dias, Ugo Silva. III. Universidade Estadual de Campinas. Faculdade de Engenharia Elétrica e de Computação. IV. Título.

Título em Inglês: Caracterização dos parâmetros de desvanecimento da distribuição alfa-mu: medidas e estatísticas
Palavras-chave em Inglês: Wireless communications systems, Radio - Transmitters and transmission - Fading, Digital communications
Área de concentração: Telecomunicações e Telemática
Titulação: Mestre em Engenharia Elétrica
Banca examinadora: Omar Carvalho Branquinho, Paulo Cardieri
Data da defesa: 22-12-2011
Programa de Pós Graduação: Engenharia Elétrica

COMISSÃO JULGADORA - TESE DE MESTRADO

Candidato: Aravind Krishnan

Data da Defesa: 22 de dezembro de 2011

Título da Tese: "On the Fading Parameters Characterization of the alpha-mu distribution: Measurements and Statistics "

Prof. Dr. Michel Daoud Yacoub (Presidente): _____

Prof. Dr. Omar Carvalho Branquinho: _____

Prof. Dr. Paulo Cardieri: _____

Resumo

Título: Caracterização dos Parâmetros de Desvanecimento da Distribuição Alfa-Mu: Medidas e Statísticas

Esta tese apresenta os resultados de medidas de campo conduzidas na freqüência de 5.5 GHz, com o objetivo de caracterizar os parâmetros do modelo de desvanecimento alpha-mu. Mais especificamente, uma quantidade de situações é investigada para se determinar a densidade de probabilidade e a função de autocorrelação destes parâmetros. O range de valores possíveis são então sugeridos baseado nos dados empíricos. Adicionalmente, as variações instantâneas da magnitude dos parâmetros correspondentes são mostradas em função do deslocamento do receptor ao longo do percurso. Os resultados provêem informações importantes sobre a utilidade prática do modelo alpha-mu mostrando, em seguida, que as estatísticas do sinal recebido se distanciam bem daquelas dos modelos conhecidos.

Palavras-chave: distribuição α-μ, caracterização de canal sem fio, parâmetros de desvanecimento, medições de campo.

Abstract

This thesis presents the results of field trial measurements conducted at a frequency of 5.5 GHz in order to characterize the parameters of the α-μ fading model. More specifically, a number of situations are investigated in which the probability density function and the autocorrelation function of these fading parameters are described. The ranges of possible practical values of the parameters are then suggested as an outcome of the empirical data. In addition, the instantaneous magnitude variations of corresponding parameters are shown as a function of the receiver position along the path. The results provide important information about the practical usefulness of the α-μ fading model, showing, in addition, that the received signal statistics greatly departs from the well known statistical models.

Keywords: α-μ distribution, channel characterization, fading parameters, field measurements.

Acknowledgements

I am heartily thankful to my supervisor, Prof. Michel Daoud Yacoub, whose encouragement, guidance and support from the initial to the final level enabled me to develop an understanding of the subject without which it would not have been possible to write this masters thesis.

The good advice, support and friendship of my co-supervisor, Dr.Ugo Dias Silva, has been invaluable on both an academic and a personal level, for which I am extremely grateful.

Words are not enough for the gratitude that I owe to my parents, who have given me their unequivocal support throughout my life.

I would like to thank my *WissTek* colleagues for their kindness, friendship and support.

I acknowledge all my friends from UNICAMP for their friendship and in particular Rogério Esteves Salustiano for his help and advice.

Special thanks goes to my housemates from *república - Sapecasa* for their friendship and companionship.

I would like to acknowledge the academic and technical support, of all the faculty members and staffs of the Post Graduate Commission (CPG) of UNICAMP.

I would like to thank my dear girlfriend, Paola, for her unconditional support, love and confidence.

Last but not least, I would like to thank CNPq for its financial support.

To my parents, teachers and the gods.

Contents

List of Figures

List of Acronym

AC	-	Alternating Current
ACF	-	Auto Correlation Function
AFD	-	Average Fade Duration
BW	-	Band Width
CC	-	Co-relation Coefficient
CCC	-	Cross Co-relation Coefficient
CDF	-	Cumulative Distribution Function
CPG	-	Post-Graduate Commission
CW	-	Continuous Wave
DECOM	-	Department of Communications
FFT	-	Fast Fourier Transform
FEEC	-	Faculty of Electrical and Computer Engineering
GPIB	-	General Purpose Interface Bus
LCR	-	Level-Crossing Rate
LNA	-	Low Noise Amplifier
PDF	-	Probability Density Function
RF	-	Radio Frequency
RMS	-	Root Mean Square
RX	-	Receiver
TX	-	Transmitter
UNICAMP	-	State University of Campinas
USB	-	Universal Serial Bus
VBW	-	Video Band Width

List of Symbols

M	-	Number of diversified branches
$F_A(\cdot)$	-	CDF of the random variable A
$f_A(\cdot)$	-	PDF of the random variable A
$P_r(\cdot)$	-	Probability of an event
m	-	Fading parameter of Nakagami-m distribution
α and μ	-	Fading parameter of the α-μ distribution
κ and μ	-	Fading parameter of the κ-μ distribution
X	-	In-phase component of a signal
Y	-	Quadrature component of a signal
$E(\cdot)$	-	Mean of the a random variable
$Var(\cdot)$	-	Variance of a random variable
$Cov(\cdot)$	-	Co-variance of a random variable
R	-	Envelope of the α-μ signal
$\hat{r}$	-	RMS value of R in κ-μ or the α^th root of R in α-μ
$\hat{r_i}$	-	The ${\alpha_i}^th$ root of $R_i^{\alpha_i}$
δ	-	Cross Co-relation Coefficient
ρ	-	Co-relation Coefficient
ζ	-	Mean angle of arrival
$\bar{T}$	-	Delay Spread
ϕ	-	Angle of incident power
ω_D	-	Maximum Doppler shift in rad/s
f_m	-	Maximum Doppler shift in Hz
λ	-	Wavelength
A_R	-	Envelope ACF of α-μ
$\hat{A}_R$	-	Empirical ACF of α-μ
f_aq	-	Data acquisition frequency
ϵ	-	Mean absolute error

Publications by the Author

1. C.L.Selvati, A.Krishnan, U.S.Dias, M.D.Yacoub. "On the Fading Parameters Characterization of the α-μ Distribution: Measurements and Statistics". *XIX Simpósio Brasileiro de Telecomunicações* (SBrT 2011), Curitiba, Parana, Brasil October 2011.

2. A.Krishnan, C.L.Selvati, U.S.Dias, M.D.Yacoub. "On the Statistics of the Fading Parameters of the α-μ Distribution: Field Trials and Validation". *The Eighteenth Annual National Conference on Communications* (NCC-2012), IIT Kharagpur, India. February 2012 (*Accepted*).

Chapter 1

Introduction

Wireless communications has become the backbone of communication. High speed, reliable and secure communication is the present day need. Providing this can be quite challenging not only because of the noise, interference and other channel impediments but these impediments change over time in unpredictable ways due to user movement [2] .

1.1 The Wireless Medium

The propagation of energy in mobile radio environment is strongly influenced by several factors including the natural and artificial relief, propagation frequency, antenna heights, and others. A precise characterization of the signal variability in this environment constitutes a hard task. Deterministic methods, such as those described by the *free space, plane earth, knife-edge diffraction and etc.* propagation models [3, 4, 5] are restricted to very simple situations Figure 1.1. They are useful, however, in providing the basic mechanism of propagation. Empirical methods, such as those used for radio-coverage planning (eg. Okumura-Hata [6], Lee [5], MBX [7]) use curves and/or formulas based on field measurement. Some of these include those deterministic solutions modified by various correction factors, to account for propagation frequency, antenna hight, polarization, type of terrain and etc. However, due to the random characteristics of the mobile radio signal, a single deterministic treatment of this signal will certainly lead the problem to a simplistic solution. More accurately, we may treat the mobile radio signal on a statistical basis, and interpret the phenomena with which it is implicated as random events occurring with a given probability. The empirical prediction methods of field measurements yield the mean values of the signal. The information provided by the mean value is essential and certainly useful, but the mean value constitutes only part of overall quality measure. For instance, it may be possible to have identical figures for the signal mean value in different environments, with the variability of the instantaneous signal leading the system to perform differently in

there environments. Therefore, for better overall performance assessment, a measure of reliability, or equivalently, outage probability, must be included, and the use of the appropriate distribution in such a case is certainly of paramount importance.

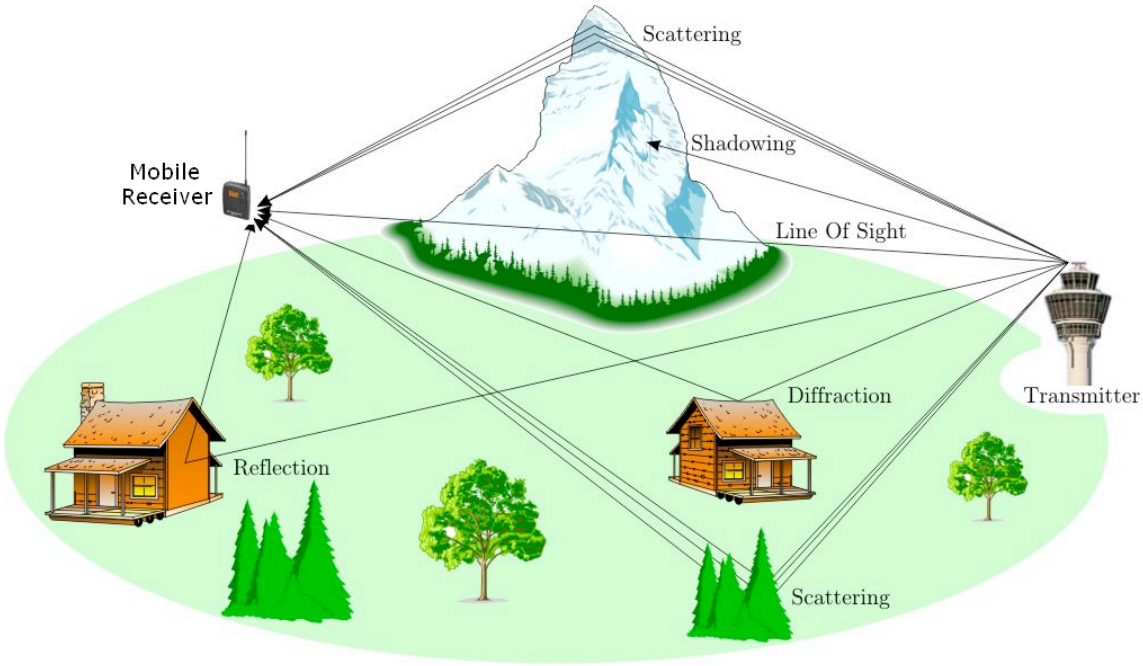

Fig. 1.1: Multi-path propagation [1]

1.2 Fading Distributions

A great number of distributions exists that well describes the statistics of the mobile radio signal. Extensive field trials have been used to validate these distributions, and the results show very good agreement between measurements and theoretical formulas. The long-term signal variation is well characterized by the log-normal distribution, whereas the short-term signal variation described by several other distributions, such as Rayleigh, Rice, and Nakagami. It is generally accepted that the path strength at any delay is characterized by the short-term distribution over a spatial dimension of a few hundred wavelengths, and by the log-normal distribution over areas with a dimension that is much larger [8]. Three other distributions attempt to describe the transition of the path strength from the local distribution to the global distribution, combining both fast and slow fading. These composite (or mixed) distributions assume the local mean, which is the mean of the fast-fading distribution, to be log-normally distributed. The best know composite distributions are Rayleigh-log-normal, also known as Suzuki, Rice-log-normal, and Nakagami-log-normal. Now, we will briefly discuss about some of these fading distributions.

1.2.1 The Rayleigh Distribution

This model is based on a statistical distribution presented by Lord Rayleigh and uses a simple fading model. In this the signal is composed of scattered waves and its quadrature components consist of zero mean and equal variance [9]

1.2.2 The Rice Distribution

When the scattered wave overlap a line of sight condition, the signal follow the Ricean distribution, in which the components have arbitrary mean and equal variance. This model was studied and presented by S. O. Rice [10].

1.2.3 The Hoyt Distribution

In this fading model, the mean of the quadrature components are unity and variances are arbitrary. The statistical model for this distribution was developed by R. S. Hoyt [11].

1.2.4 The Nakagami Distribution

This model consists of a signal composed of various clusters, where each cluster follows the Rayleigh model. This type of fading distribution was analyzed and was extensively used in fading channel characterization by M. Nakagami [12].

1.2.5 The κ-μ Distribution

A generalization of the Ricean and Nakagami fading models, this model describes the signal which is composed of Ricean clusters or the clusters in which the quadrature components have arbitrary mean and equal variances. This is an interesting model by the fact that it does not assume identical statistical properties for all the clusters of the signal, but the mean may vary from one cluster to other [13].

1.2.6 The η-μ Distribution

In this fading model, each of its cluster follows the Hoyt model, that is, its quadrature components have zero mean and arbitrary variance. Therefore, Hoyt and Nakagami are special cases of the η-μ fading model [14].

1.2.7 The α-μ Distribution

The α-μ distribution is a general fading distribution that includes various models like the Gamma (and its discrete versions Erlang and central Chi-squared), Nakagami-m (and its discrete version Chi), exponential, Weibull, one-sided Gaussian, and Rayleigh that can be observed directly from α-μ. With the aim at exploring the nonlinearity of the propagation medium, a general fading distribution the α-μ distribution was proposed [15]. This distribution was thought to be new, but it is, in fact, a rewritten version of the generalized Gamma distribution (at the time unknown to the author), which was first proposed by Stacy [16]. The α-μ distribution is general, flexible, and has easy mathematical tractability. Its density, cumulative frequency, and moments appear in simple closed-form expressions. All these features combined make the Stacy or α-μ distribution very attractive. Using the fading model as proposed in [15], a deeper characterization of the Stacy or α-μ distribution can be achieved. The flexibility and applicability of the α-μ fading model have been recognized in practice. Field measurements carried out in diverse instances show that in many situations and in different scenarios the α-μ model better accommodates the statistical variations of the propagated signal [17, 18, 19, 20, 21].

1.3 First and Higher Order Statistics

In radio channel characterization the first order statistics usually deals with the mean, variance, the PDFs (Probability Density Function) and the CDFs (Cumulative Distribution Function). Higher order statistics deal with the ACFs (auto-correlation function), Auto-covariance functions and etc., all of which will be presented and discussed in this thesis.

1.4 Work Plan

In this thesis, the empirical probability density functions (PDF) and the autocorrelation functions of α and μ, which are the fading parameters of the α-μ distribution, are obtained based on field measurements. In addition, the ranges of possible practical values assumed by α and μ are estimated from the empirical data and their instantaneous magnitude variations are evaluated considering the displacement of the mobile received in outdoor environments. Since the values of α and μ are indicators of the nonlinearities and multi-path clustering of the radio channel, the knowledge of their PDFs, autocorrelations, and magnitude ranges, can be used in the evaluation and design of different wireless communications techniques, such as diversity combining techniques, adaptive modulation schemes, modeling and analysis of interferences, outages probabilities, design and simulation of adaptive antennas systems, among others.

1.5 Thesis Structure

The remainder of this work is structured as follows.

- **Chapter 2-** In this chapter the α-μ fading model is revisited. The fading model is explained, its statistics are given and the moment based estimator is provided for the same.
- **Chapter 3-** In chapter 3, the field measurement vehicle's configuration is discussed in detail.
- **Chapter 4-** In chapter 4, field trials and measurements are conducted in order to investigate first and higher-order statistics of the α and μ fading parameters. The empirical Probability Distribution Functions (PDFs) and Autocorrelation Functions (ACFs) of the α and μ fading parameters are presented and discussed based on the measurement campaigns. The mean, median and standard deviation values are found out and presented. Moreover, the instantaneous variation of the α and μ magnitudes are also obtained with distance and analyzed, and the practical value ranges of α and μ parameters are estimated.
- **Chapter 5-** Finally, in Chapter 5, conclusion remarks and future work possibilities are presented.

Chapter 2

The α-μ Distribution Revisited

Several well-known fading distributions have been derived assuming a homogeneous diffuse scattering field, resulting from randomly distributed point scatterers. The assumption of a homogeneous diffuse scattering field is certainly an approximation, because the surfaces are spatially correlated characterizing a nonlinear environment [22]. With the aim at exploring the nonlinearity of the propagation medium, a general fading distribution the α-μ Distribution was proposed in [15].

2.1 The α- μ Fading Model

The α-μ distribution is a general fading distribution that can be used to better represent the small-scale variation of the fading signal in a non line-of-sight fading condition. It includes as special cases important other distributions, such as Nakagami-m, and Weibull. (Therefore, One-Sided Gaussian and Rayleigh are also special cases of it). As its name implies, it is written in terms of two physical parameters, namely α and μ. The power parameter $\alpha > 0$ is related to the non-linearity of the environment, whereas the parameter $\mu > 0$ is associated to the number of multi-path clusters [23].

For a α-μ fading signal with envelope R, an arbitrary parameter $\alpha > 0$, with the α-root mean value $\hat{r} = \sqrt[\alpha]{E(R^\alpha)}$, in which $E(\cdot)$ signifies the expectation operator, the α-μ envelope PDF is written as

$$f_R(r) = \frac{\alpha \mu^\mu r^{\alpha\mu-1}}{\hat{r}^{\alpha\mu}\Gamma(\mu)} \exp\left(-\mu \frac{r^\alpha}{\hat{r}^\alpha}\right), \tag{2.1}$$

for which $\mu > 0$ is the inverse of the normalized variance of R^α, i.e.,

$$\mu = \frac{E^2(R^\alpha)}{V(R^\alpha)}, \tag{2.2}$$

$\Gamma(\cdot)$ is the Gamma function [14, Eq. 6.1.1], and $V(\cdot)$ denotes the variance operator.

The fading model for the α-μ distribution considers a signal composed of clusters of multi-path waves propagating in a nonhomogeneous environment. Within any one cluster, the phases of the scattered waves are random and have similar delay times with delay-time spreads of different clusters being relatively large. The clusters of multi-path waves are assumed to have the scattered waves with identical powers. The resulting envelope is obtained as a nonlinear function of the modulus of the sum of the multi-path components. Such a nonlinearity is manifested in terms of a power parameter, so that the resulting signal intensity is obtained not simply as the modulus of the sum of the multi-path components, but as this modulus to a certain given exponent. The author of [23] conjectures that the resulting effect on the received signal propagated in a certain medium is manifested in terms of a nonlinearity [23]. Figures 2.1 and 2.2 present some example theoretical plots of the density functions with different values of α and μ and compared with other models.

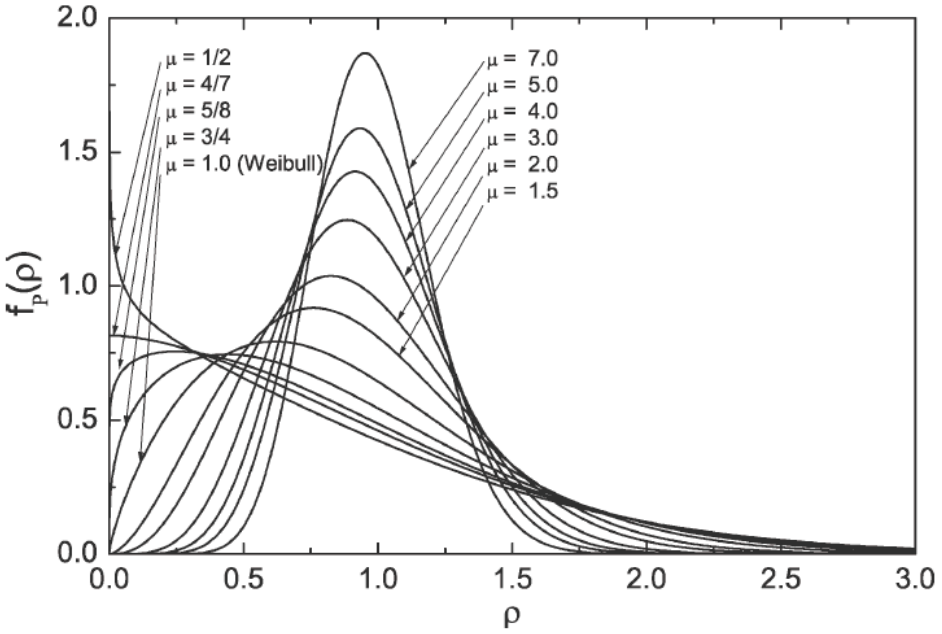

Fig. 2.1: Various shapes of the α-μ density function for α = 7/4 compared with Weibull.

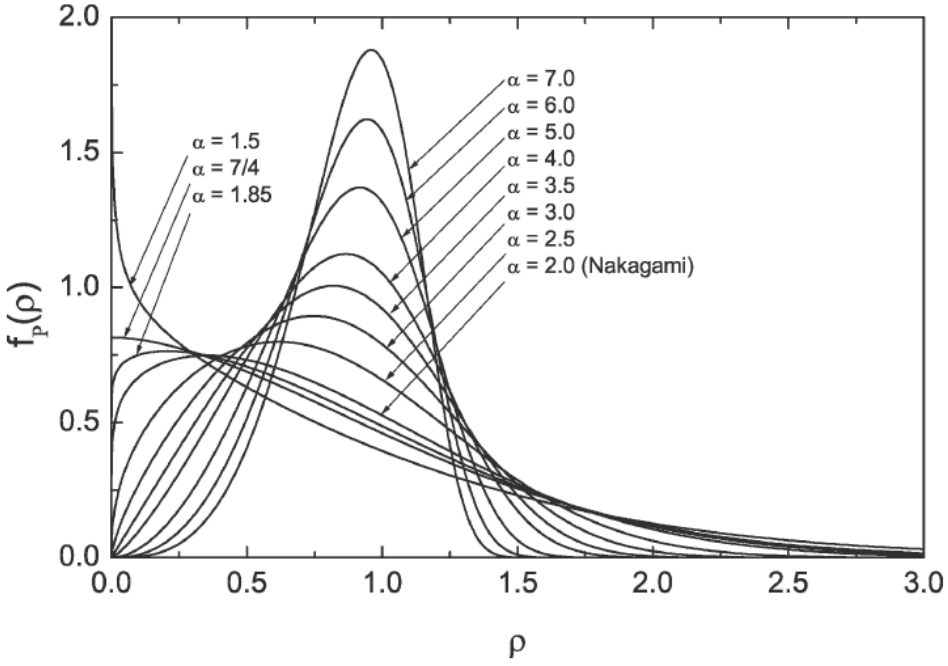

Fig. 2.2: Various shapes of the α-μ density function for μ = 4/7 compared with Nakagami.

2.2 The Moment-Based α-μ Estimator

The moments of the α-μ envelope are given as $E[R^k] = \frac{\hat{r}\Gamma(\mu+k/\alpha)}{\mu^{k/\alpha}\Gamma(\mu)}$. From this, an equality is defined that is useful for the estimation of the parameters of this distribution

$$\frac{E^2[R^\beta]}{E[R^{2\beta}] - E^2[R^\beta]} = \frac{\Gamma^2(\mu + \beta/\alpha)}{\Gamma(\mu)\Gamma(\alpha + 2\beta/\alpha) - \Gamma^2(\mu + \beta/\alpha)}, \tag{2.3}$$

in which β is chosen arbitrarily. For two distinct and arbitrary values of β, two equations are set up so that the physical parameters α and μ are encountered. Now, as given in the section VI of [23] for a particular case in which β = 1 and β = 2, Eq. 2.3 yields an estimator in terms of the first and second moments. Of course, from Eq. 2.3, other moment-based estimators can be used.

2.3 Higher Order Statistics

Some higher order statistics are described below (although not used in this thesis, we briefly describe them for our understanding).

2.3.1 Correlation Coefficient

The generalized correlation coefficient $\delta_{p,q}$ of two α-μ variants R_1 and R_2 can be defined from [23] as

$$\delta_{p,q} = \frac{C(R_1^p, R_2^q)}{\sqrt{V(R_1^p)V(R_2^q)}} = \frac{C(P_1^p, P_2^q)}{\sqrt{V(P_1^p)V(P_2^q)}} \tag{2.4}$$

where C(.,.) is the covariance operator.

2.3.2 Level-Crossing Rate (LCR) and Average Fade Duration (AFD)

Level-crossing rate $N_R(r)$ and the average fade duration $T_R(r)$ are important second-order statistics, from [23], they are defined as

$$N_R(r) = \int_0^\infty \dot{r} f_{\dot{R},R}(\dot{r}, r) d\dot{r} \tag{2.5}$$

where $f_{\dot{R},R}(.,.)$ is the joint PDF of two envelopes. The AFD is defined as the mean time during which the received envelope remains below a given threshold r_i, after crossing in the negative direction, which can be expressed as

$$T_R(r) = \frac{F_R(r)}{N_R(r)}. \tag{2.6}$$

where $F_{R_i}(.)$ is the Cumulative Distribution Function (CDF) of R_i.

There are at least two ways to obtain these statistics. The first, through statistical knowledge corresponding to the channel from which the α-μ distribution can be obtained e.g., Nakagami-m. The second through mathematical description of the physical phenomenon understood by the model in question. Both, of course, lead to the same result. In [23] the second method was used to obtain the LCR and the AFD, such that,

$$N_R(r) = \frac{\omega \mu^{(\mu-0.5)} \rho^{(\mu-0.5)}}{\sqrt{2\pi}\Gamma(\mu)\exp(\mu\rho^\alpha)} \tag{2.7}$$

$$T_R(r) = \frac{\sqrt{2\pi}\Gamma(\mu, \mu\rho^\alpha)\exp(\mu\rho^\alpha)}{\omega \mu^{(\mu-0.5)} \rho^{(\mu-0.5)}} \tag{2.8}$$

where $\rho = \frac{r}{\hat{r}}$ is the Doppler shift in rad/s. For α = 2, Eqs. 2.7 and 2.8 are reduced to Nakagami-m [18, Eqs. (17) and (21)], respectively. For μ = 1, Eqs. 2.7 and 2.8 are reduced to Weibull [19, Eqs. (12) and (13)].

Chapter 3

Field Measurement System

In this chapter we introduce the field measurement system setup. This setup can generate continuous Radio-Frequency signal waves using a fixed transmitter and collect spacial sample with a mobile reception vehicle. The overall system fulfils the needs for the experimental validation of the first and second order statistics in this work. The technical specifications are described in Appendix B.

3.1 Transmitter

The overall configuration of the transmitter is explained in the diagram in Figure 3.1. This was designed to work with more than one RF signal generator although, for our experiments specifically only one RF signal generator was used. The 5.5 GHz frequency has been chosen because of its use in the non-licensed radio limits.

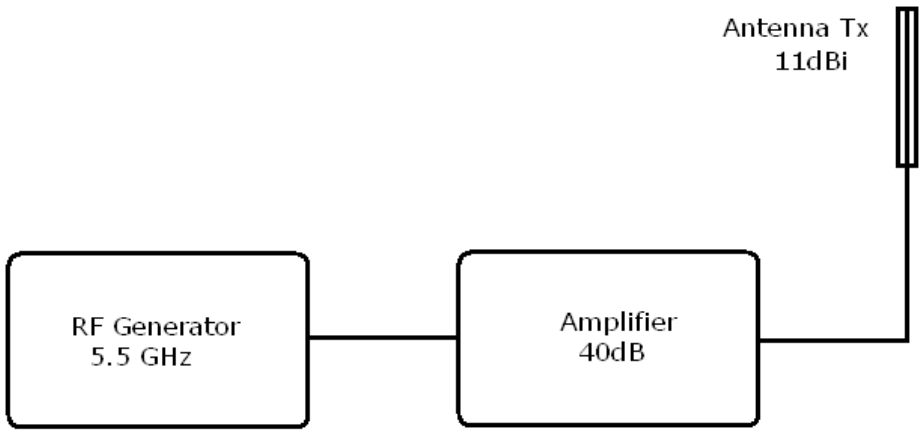

Fig. 3.1: Transmitting antenna

Of course, all the setup devices (antennas, cables, connectors and etc.) are chosen to operate in the

given frequency. In the case of the outdoor transmitter, the system is configured to obtain a effective radiated power upto 20 W(43dBm).

Note that the transmitter can be installed in the terrace of the buildings for outdoor transmission or inside the buildings for indoor transmission. This gives an excellent flexibility to realize the field measurement campaigns in various types of environments. The only difficulty here is the logistics of the installation of the equipments, which is normal and understandable in this kind of experiments.

3.2 Data Acquisition Setup

The method of data acquisition received some important changes from the field measurement system proposed in [24]. It was completely reconfigured - the radio system, signal analyzer, data acquisition and post processing program and energy.

The equipment is divided in four independent parts, according to the block diagram show as Figure 3.2: Low Noise Amplifier, Spectrum Analyzer, Data collector (using the GPIB-USB cable connected to the spectrum analyzer) and Energy.

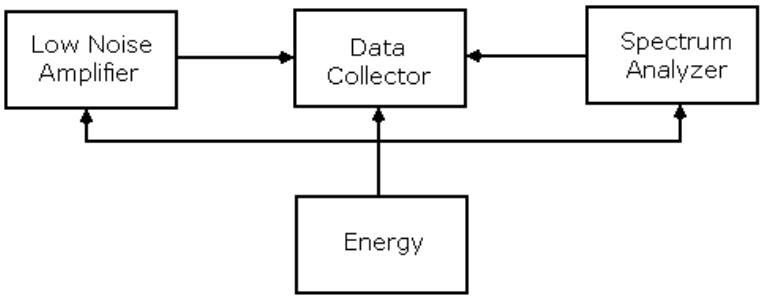

Fig. 3.2: Mobile Reception System Block Diagram

First, the system is configured with a particular spacial sampler. With each valid phase inside this sample, the level of signal is verified using the signal analyzer. Next, the information from both blocks (samplers and analyzers) are stored using a data collection cable (GPIB-USB) connected to the spectrum analyzer to be processed later. Due to its construction, the field measurement vehicle allows other configuration by replacing/adapting the modules

Receiving Antennas

Consists of monopole antennas and omnidirectional antennas coupled to a plane fixed to the data acquisition set. RF signals received by these antennas are referred to the variable attenuators.

Amplifiers / Variable Attenuators

The function of the amplifiers / variables attenuators is to maintain the level of signal received at the linear part of the operating range of the equipments, which varies from -122 dBm to -47 dBm. The low noise amplifier (LNA) is selected for the systems as specified in Appendix B. In the case of measurements occurring near the transmitter, there is a need to introduce some level of attenuation, although never more than 20 dB just not to compromise the noise figure and dynamic range of operation of the amplifier/ variable attenuator.

The CW signals received by the antenna, after passing through the attenuators and amplifiers, are engaged in sequence into the spectrum analyzers.

Spectrum Analyzers

There are certain requirements that are important to the specifications of this measuring equipment, such that it can operate in the frequency bands of the transmitted carrier, it needs to be robust to variations in temperature and also have good resistance to mechanical vibrations arising due to the movement of the vehicle during the campaigns field measurements.

The following parameters: the frequency range (span), scan time (sweep time), video bandwidth (VBW) and bandwidth (BW):

- The span was set to 0 Hz. Thus, the device operates as an oscilloscope (receiver), measuring the power of a single carrier.
- The sweep time was set at the lowest possible value. Thus, it may be a sign displayed on the screen in the form of a line segment, since we are not providing enough time for changes in signal levels before it is fully drawn. A suitable value for the sweep time is 15 ms.
- The BW and VBW are parameters that define the format of the internal filters of the analyzers. The smaller the selected values, the lower the bandwidth of these filters and therefore less noise will be captured by the equipment, on the other hand, it increases the sensitivity with respect to temperature changes, since the temperature variation can affect the center frequency of the filters in test. That is, the selection of the values are directly correlated to the range of power values that each data acquisition equipment can measure, which, in turn, depends on the models of analyzers used. The best values common to the models used were 10 Hz to 30 kHz for the VBW and BW, respectively.

The collection of the measured data by the analyzer was made through GPIB-USB cable. Each output provides a voltage that represents the amplitude of the signal shown on the screen. The amplitude, in turn, is proportional to the measured power level. It is sufficient, therefore, to determine

this ratio and then set the reception power of each carrier. Finally, the video outputs of each spectrum analyzer is connected to the data acquisition board.

3.2.1 Data Collector

This part of the reception vehicle is responsible for acquiring and storing the measurement. It consists of two parts: a GPIB-USB cable connected to the spectrum analyzer and a laptop computer.

Data Acquisition Method

We basically used a GPIB-USB cable connected to the spectrum analyzer and the laptop to collect the data. Our main aim was that the frequency of operation of this unit should be able to keep track with the production of pulses generated by the sprocket, with the movement of the data acquisition equipment, as considerations made in Section 3.2.1.

Computer and Data Acquisition Program

There is no particular specifications for the laptop computer. Any simple model which is able to run a Java virtual machine can be used. The Data acquisition program's function is to read the samples collected by the acquisition board and record the same in text files that allow to process it further.

3.2.2 Energy

This block is designed to supply power to the other blocks, sampler, data collector and signal analyzers. The main intention is to remain self-sufficient in the area of energy and provide support for a minimum number of hours required. A very light weight inverter 300 W of power was used. Thus, the computer receives AC power through the inverter and other equipment are supplied the DC power directly from two batteries. This method resulted in an average range of seven working hours.

3.3 Conclusions

The field measurement system was configured successfully to operate with multiple RF signals. The transmitter and the reception vehicle together showed good flexibility in adjustments to new settings. Although, the system could operate with multiple antennas, for the experiments of this thesis, only the single-input-single-output configuration was used.

Chapter 4

Field Trials and Validation

The aims of this chapter are;

- to estimate the value ranges of the α and μ parameter's;
- to characterize the amplitude variations with the distance of the α and μ fading parameters;
- to obtain the empirical PDFs of the α and μ parameters;
- and to obtain the empirical ACFs of the same.

4.1 Field Measurements

The system was configured to operate with a single carrier figure (3.1) which can be modified for operation with dual carrier (multi carrier) with the intention of investigating the correlation between two envelopes for future work. Higher statistics are investigated using a single carrier based on the original system configuration [24]. Follows next the configurations and field measurement techniques:

4.1.1 System Environment

The transmitter was fixed on the roof top of the Block E of the Faculty of Electrical and Computer Engineering building figure (4.1) with the following configuration:

- A signal generator operating at the frequency of 5.5 GHz with output power of 0 dBm;
- The singal generator output was directly fed in to the RF, with a gain of 40dB;
- The output of the power amplifier is coupled to a 22 cm cable, an omnidirectional antenna with a gain of 11 dBi;

Fig. 4.1: Transmitting antenna

The reception accounts for most of the differences and complexities. Thus, have a spectrum analyzer, an attenuator, a splitter and an omnidirectional antenna.

The measurement campaigns were conducted in the surroundings of the state university of Campinas, thus simulating a particular outdoor environment. The mobile reception unit moved through the surroundings at a constant speed of 30 km/h. We made sure that mild urban, sub-urban and rural environments are simulated with our selection of the roads, streets and avenues. Figure 4.2 shows the campus and its surroundings where the field measurement were conducted.

We conducted our trials at nine different locations as shown in Figures 4.3 to 4.8. The same methodology was followed to take all the measurement. Some of the environments were near to the transmitter, others were a few blocks away, whereas some were far away. Thus we had line of sight, presence of various kinds of vehicles,different kinds of trees, small and big buildings, people among others.

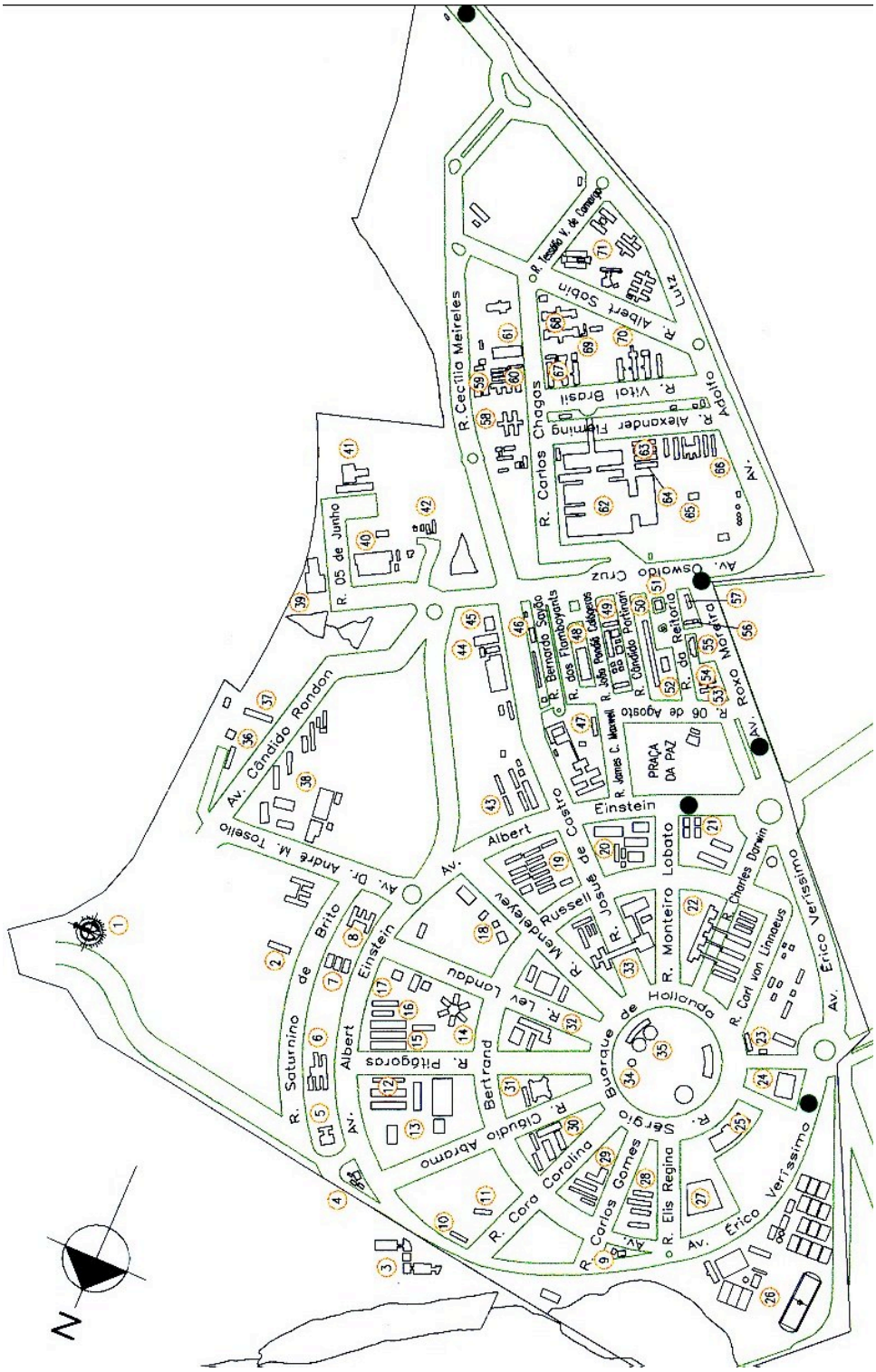

Fig. 4.2: State University of Campinas surroundings

Fig. 4.3: Rua Antonio Augusto Alemeida

Fig. 4.4: Rua Luverci Pereira De Souza

Fig. 4.5: Rua Sheiro Mori

Fig. 4.6: Rua Ruberlei

Fig. 4.7: Avenida Prof Atilio Martins 1

Fig. 4.8: Avenida Prof Atilio Martins 2

4.2 Validation

As discussed before, the data are collected in the laptop computer for post processing. The fast and slow fading were separated using a program specially written to post process the data. The number of samples depends on the environment in which the trial was conducted. In our case we used a sampling interval of λ/180, at 5.5 GHz. The envelope of each received signal is measured and using this we calculate the α and μ fading parameters thus resulting in the calculation of the statistics associated.

4.2.1 Moving Average Method

To separate the slow and fast fading, we calculated the envelopes of each file from the acquired power. Both the envelope and the received power were composed of slow and fast fading. In order to separate the slow and fast fading, we computed the Root Mean Square (RMS) values of the envelopes. Later, we divided each of these envelope values by the RMS values thus separating the fast and slow fading.

Now, from the envelope values, the α and μ fading parameters are estimated using the moment based estimators Eq.(2.3). Initially, this method seemed to be correct but later it resulted in abnormal curves with abrupt changes in values of the fading parameters. Hence, we used the moving average method to re-calculate the values of the α and μ fading parameters. We used a window length of $10,800$ for files of length varying from $120,315$ to $360,945$ envelope values. A list of α and μ fading parameters were obtained for each file, thus producing smother curves with gradual changes in the α and μ parameters as expected .

4.2.2 Mean, Median and Standard Deviation

The mean, median and standard deviation values are shown in Table/Figure 4.9,

Nos	Name of Street/Avenue	α			μ		
		Mean	Standard Deviation	Median	Mean	Standard Deviation	Median
		2,58733	1,9333	2,27264	0,90409	2,66772	0,8471
		2,24933	1,45542	2,07598	1,26554	3,5248	1,0159
1	Rua Dr Antonio Augusto	2,3189	1,2929	2,1223	1,10413	4,133	1,0005
		2,9215	1,6803	2,5995	0,65774	1,9919	0,73109
		3,1441	2,742	2,5762	0,6286	3,6129	0,7174
		2,624	1,3105	2,3963	0,8814	2,9549	0,8078
2	Rua Cora Carolina	2,9976	1,9399	2,5773	0,6961	1,7208	0,7501
		2,37115	1,59305	2,21649	1,34958	8,51982	0,964632
3	Institudo de Economia	2,99021	3,1602	2,37971	1,04067	5,43762	0,883999
		2,51648	1,45215	2,3068	1,005	3,0302	0,8962
		2,57605	1,42225	2,357	0,966411	3,07485	0,85012
		3,6668	7,7691	2,3271	2,891	8,3379	1,3117
4	Avenida Pf Atilio Martins - Downtown	2,56717	1,70804	2,28838	1,06613	4,39393	0,95328
		2,6687	1,8126	2,3138	1,0301	4,78852	0,88905
		2,22311	0,72216	2,29281	1,0499	0,63347	0,856098
5	Avenida Pf Atilio Martins - Unicamp	2,76214	1,88252	2,39714	0,857782	3,6487	0,84153
		2,40208	1,39136	2,17235	1,14289	4,86106	0,954249
		2,46605	1,3421	2,26864	1,00444	2,44323	0,87985
6	Rua Luverci Pereira De Souza	3,34308	2,50327	2,62343	0,4385	1,64841	0,69819
		2,34809	1,11421	2,2439	1,09643	3,57149	0,8759
		2,39057	1,30235	2,1964	1,07529	4,71437	0,932309
7	Rua Dr Ruberlei Boareto da Silva	2,4809	1,47673	2,28767	0,945023	2,55101	0,85794
		2,53334	1,02597	2,44949	0,83194	1,19034	0,75184
8	Praça Sérgio Buarque de Holanda	2,51425	1,5745	2,2246	0,95801	3,17795	0,92548
		2,619	1,41942	2,46052	0,87247	1,33077	0,79463
9	Rua Dr Shigeo Mori	2,41634	1,34566	2,20458	1,10971	4,39596	0,98863
	Average Values	**2,64224**	**1,86046**	**2,33196**	**1,03342**	**3,55214**	**0,88367**

Fig. 4.9: Table of Mean, Median and Standard Deviation

It can be seen from table that the average estimated median and mean values of α are respectively 2.33 and 2.64, with standard deviations of 1.86. For the μ cases, these are respectively 0.88 and 1.03, with standard deviations of 3.55. The range of possible practical values of α, as found here, vary from 1.1 to 9. And for the μ, these are from 0.1 to 6. The knowledge of possible practical levels of α and μ and their expected values are very important to better estimate the fading margin in wireless systems.

4.2.3 Probability Density Functions (PDFs)

Figures 4.10 to 4.34 present the curves of the empirical α and μ PDFs for all the nine same environments at various points of references. These empirical PDFs of both empirical α and μ have similar shapes, but they are centered in different values and they seem to approximately follows the α-μ PDF itself (physically). The plots are are shown below;

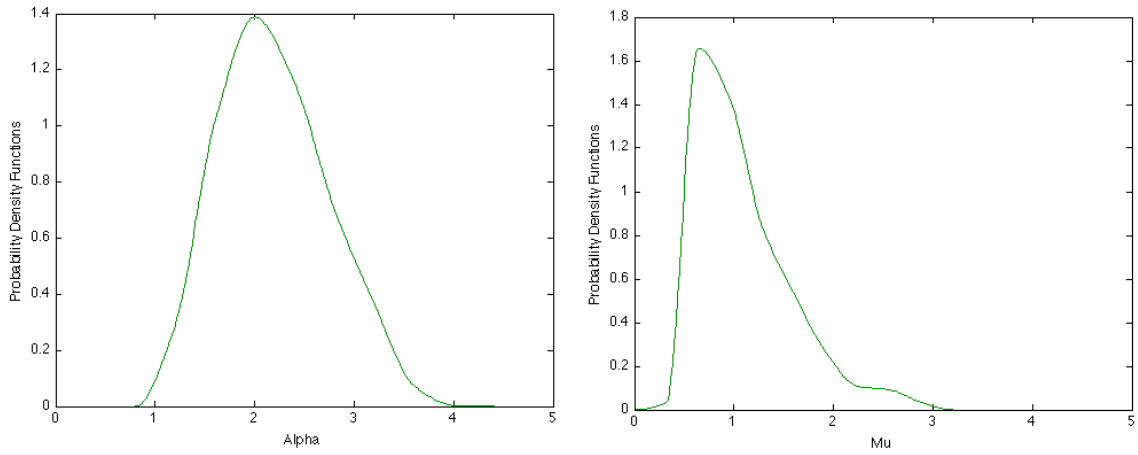

Fig. 4.10: PDF taken at Rua Luverci Pereira point 1

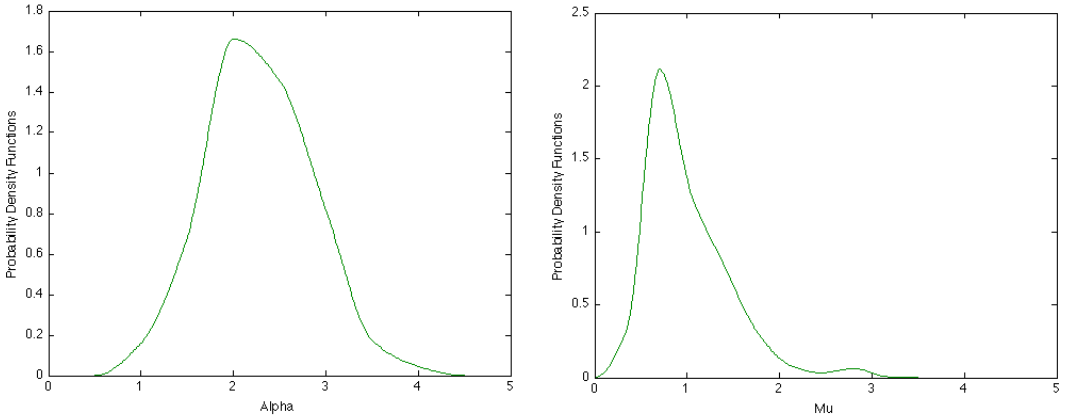

Fig. 4.11: PDF taken at Rua Luverci Pereira point 2

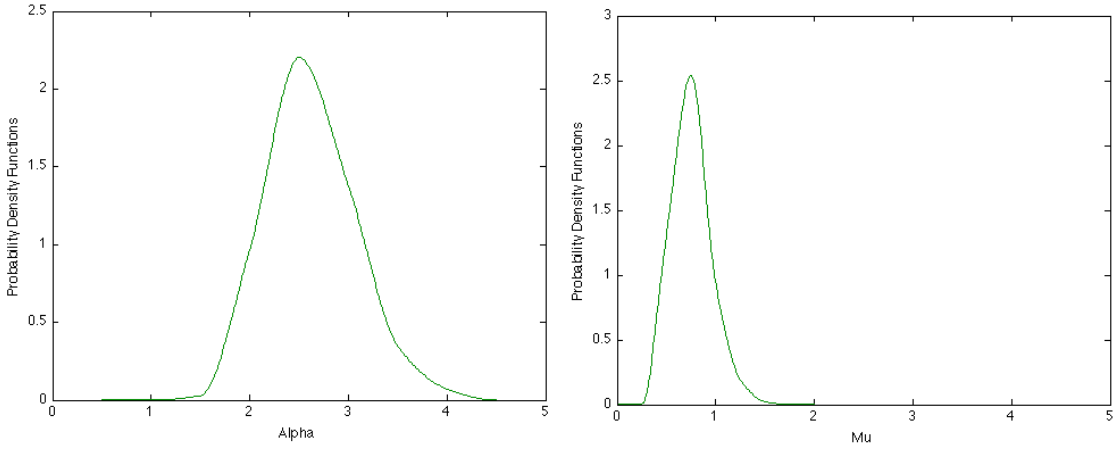

Fig. 4.12: PDF taken at Rua Luverci Pereira point 3

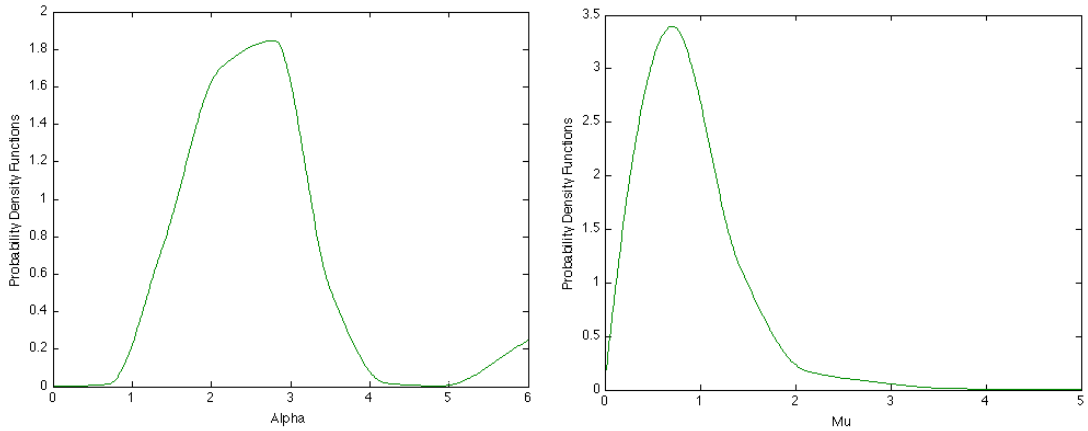

Fig. 4.13: PDF taken at Rua Shegio Mori point 1

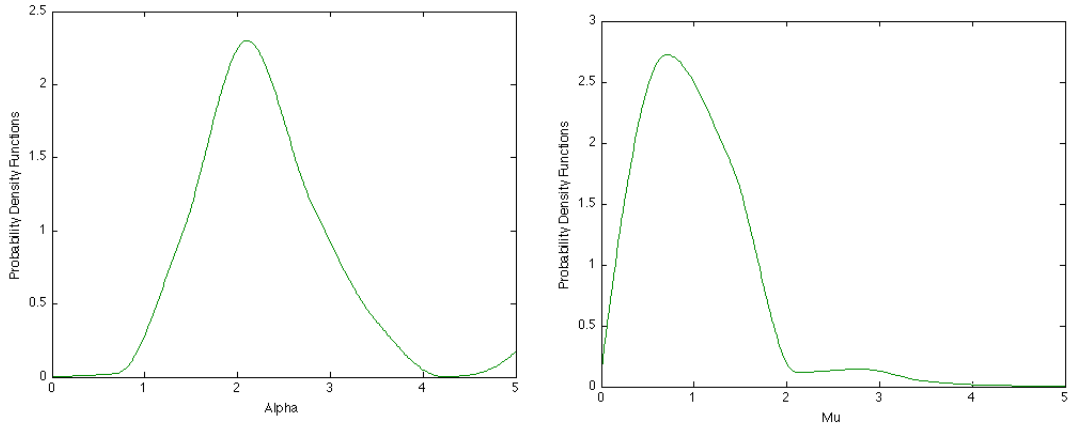

Fig. 4.14: PDF taken at Rua Shegio Mori point 2

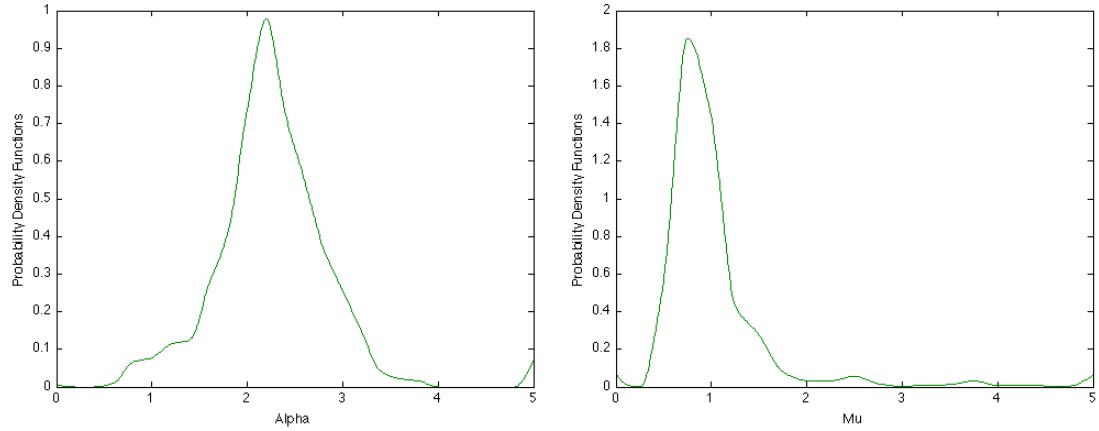

Fig. 4.15: PDF taken at Rua Ruberlei point 1

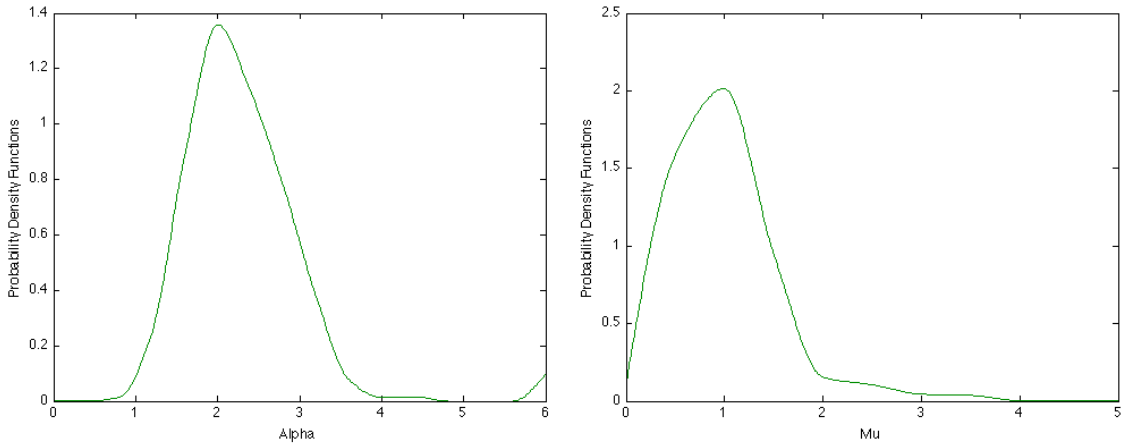

Fig. 4.16: PDF taken at Rua Ruberlei point 2

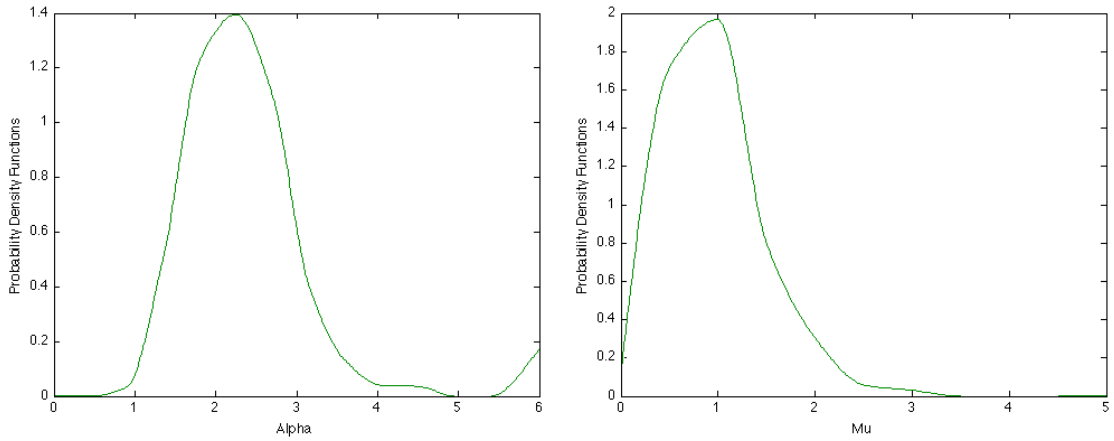

Fig. 4.17: PDF taken at Rua Ruberlei point 3

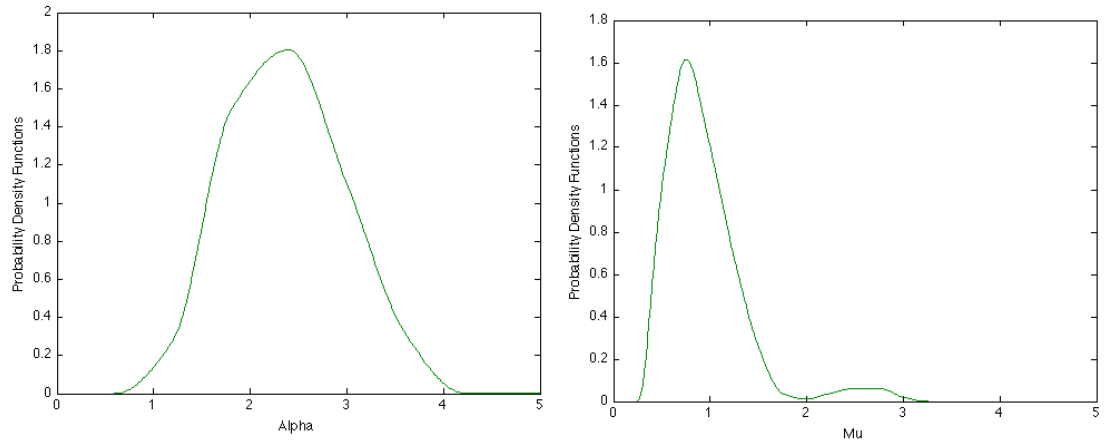

Fig. 4.24: PDF at Av Prof Atilio Martins towards Unicamp point 2

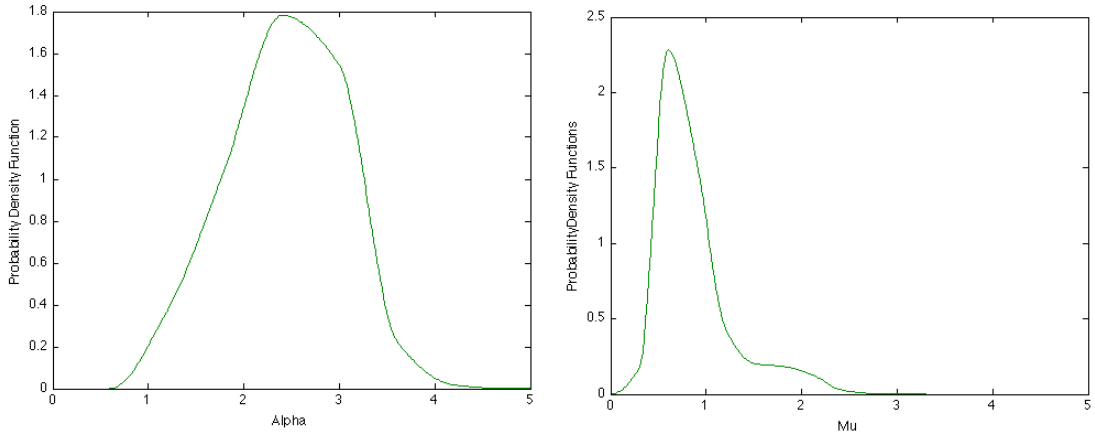

Fig. 4.18: PDF taken at Parça Sergio Buarque Holanda point 1

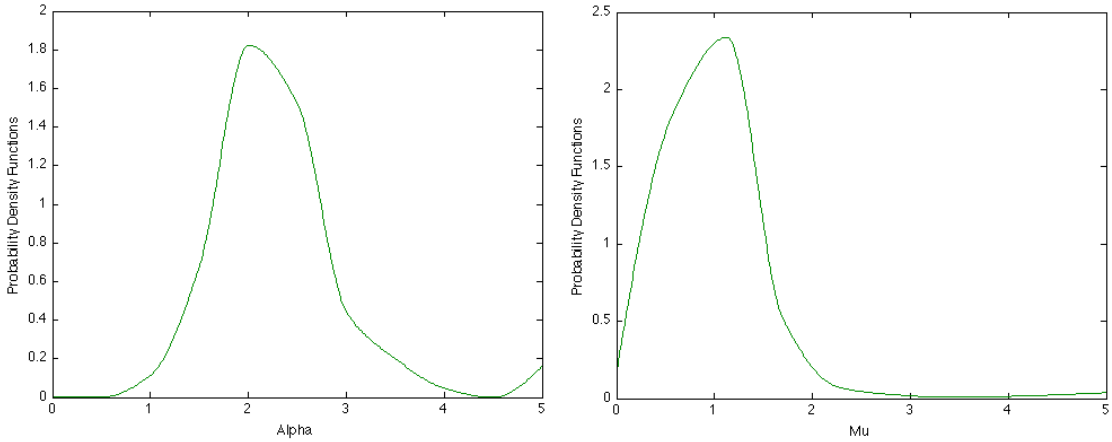

Fig. 4.19: PDF taken at Parça Sergio Buarque Holanda point 2

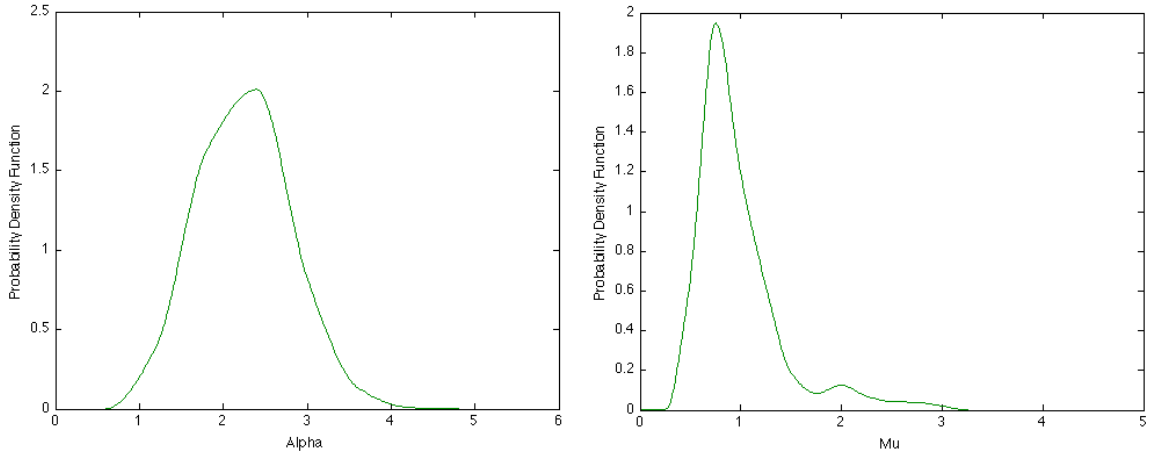

Fig. 4.20: PDF taken at Rua Antonio Augusto point 1

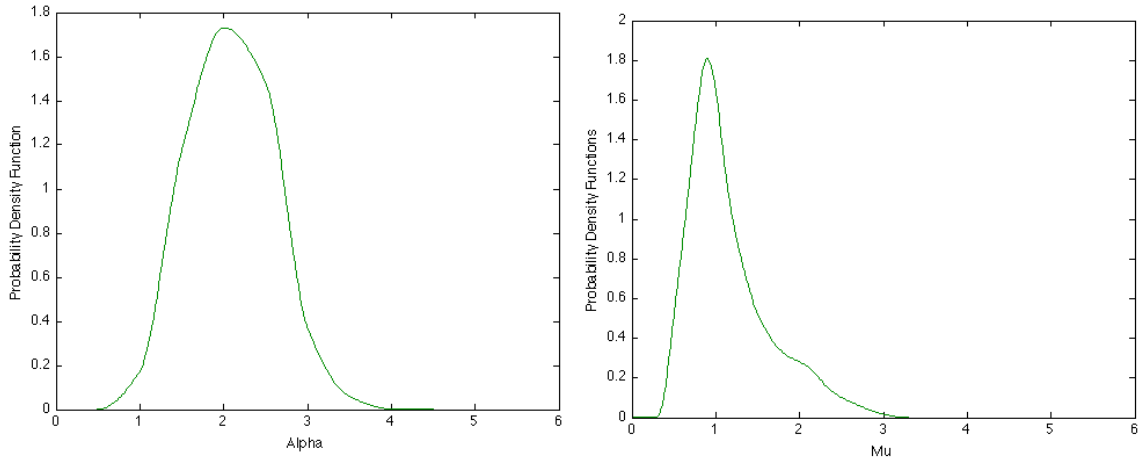

Fig. 4.21: PDF taken at Rua Antonio Augusto point 2

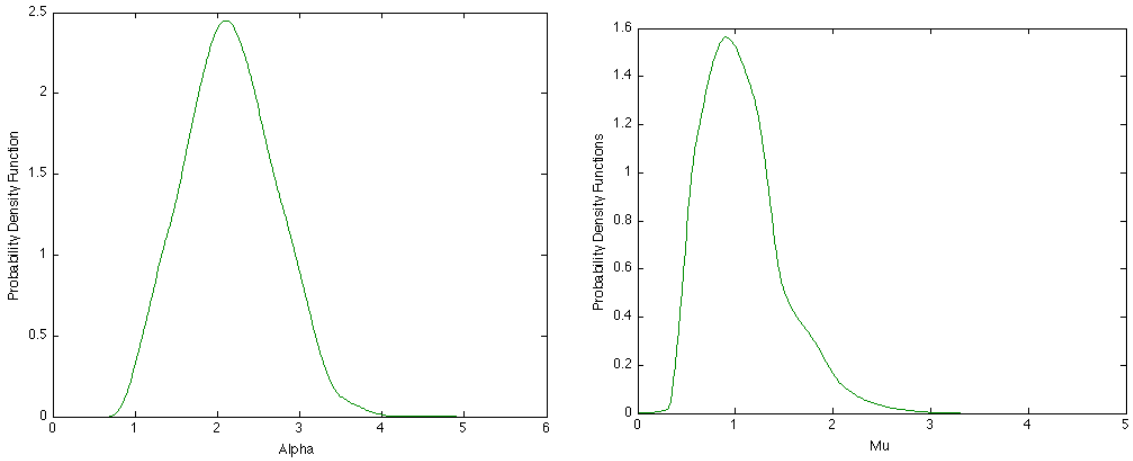

Fig. 4.22: PDF taken at Rua Antonio Augusto point 3

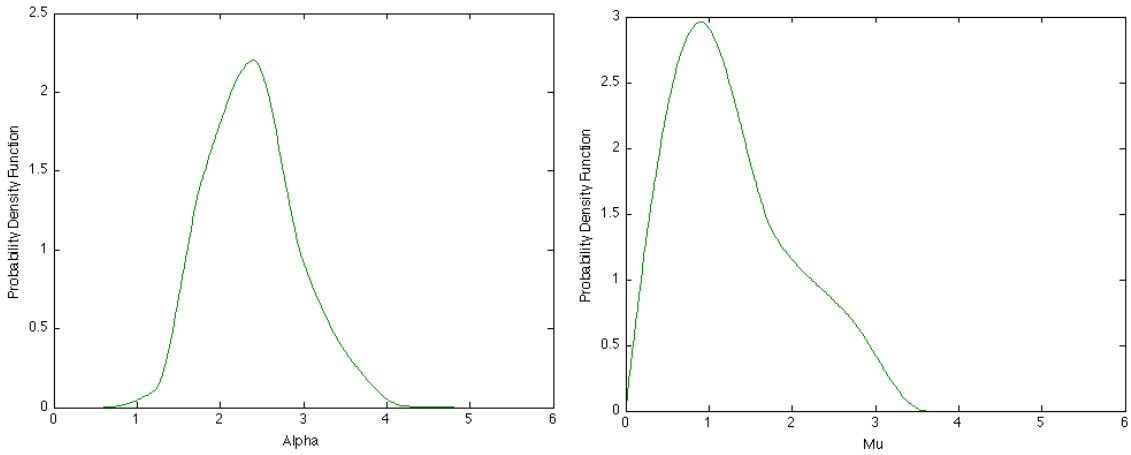

Fig. 4.25: PDF at Av Prof Atilio Martins towards Unicamp point 3

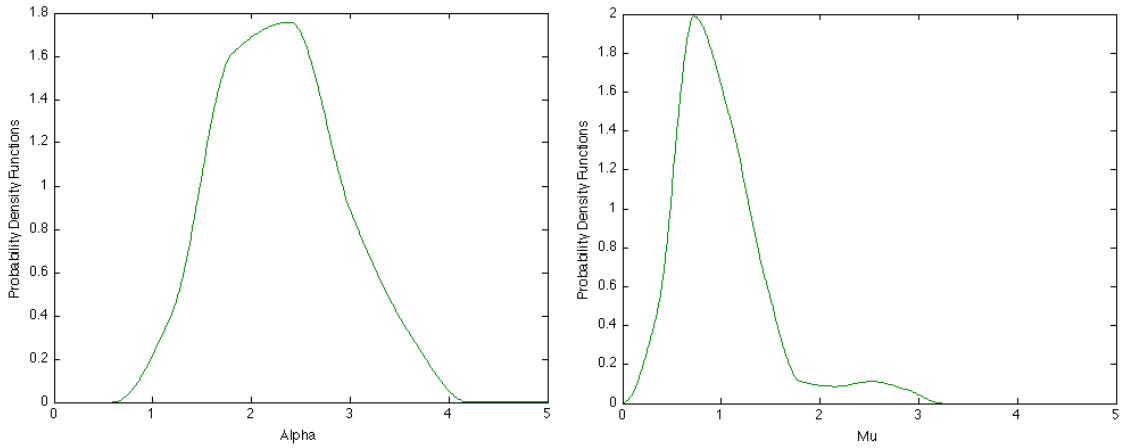

Fig. 4.23: PDF at Av Prof Atilio Martins towards Unicamp point 1

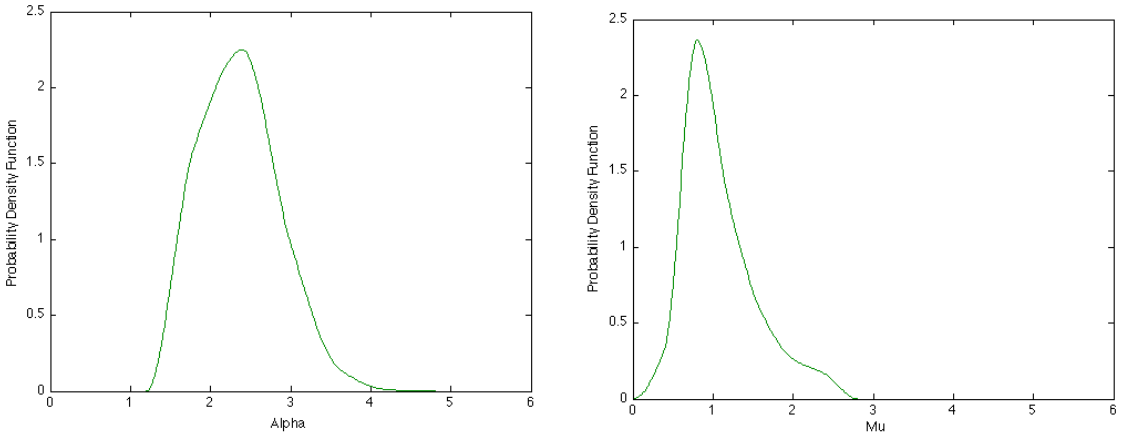

Fig. 4.26: PDF at Av Prof Atilio Martins towards Unicamp point 4

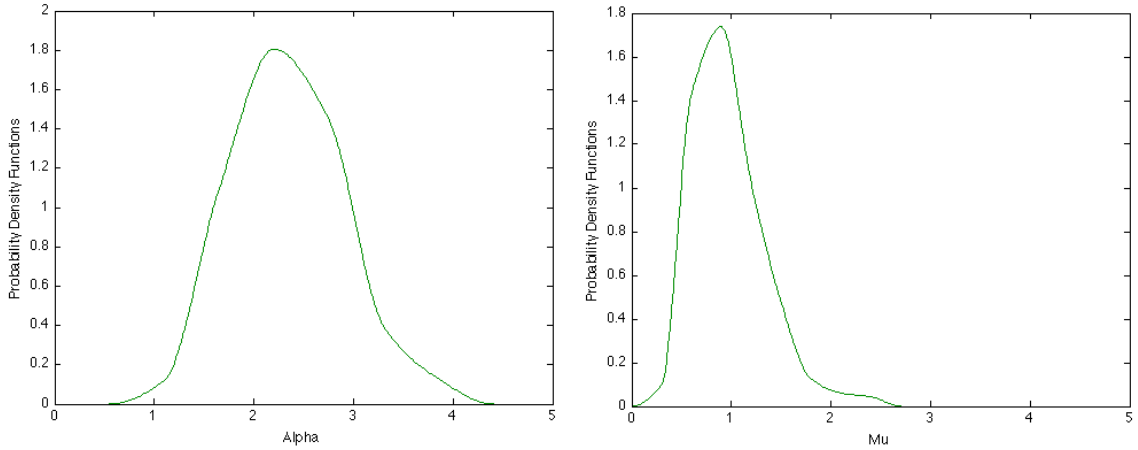

Fig. 4.27: PDF taken at Av Prof Atilio Martins towards Downtown Point 1

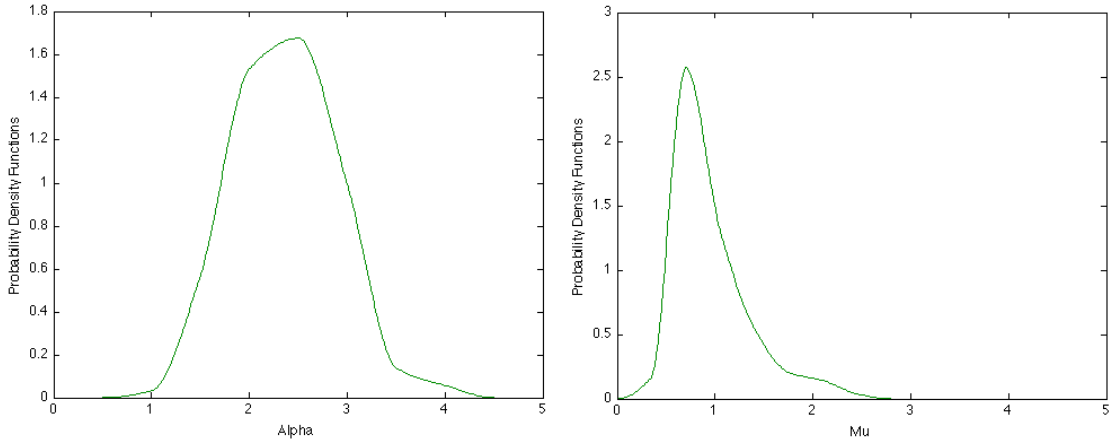

Fig. 4.28: PDF taken at Av Prof Atilio Martins towards Downtown Point 2

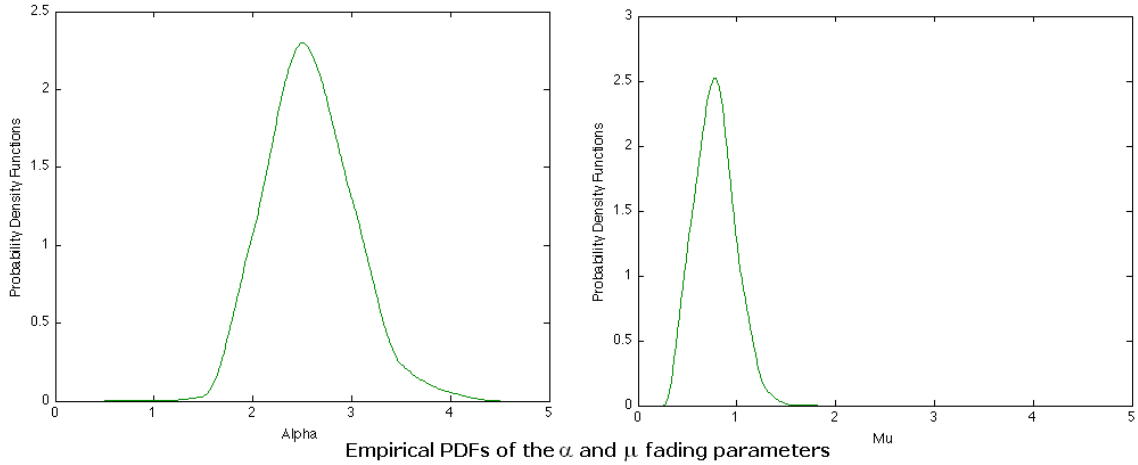

Fig. 4.29: PDF taken at Rua Cora Carolina Point 1

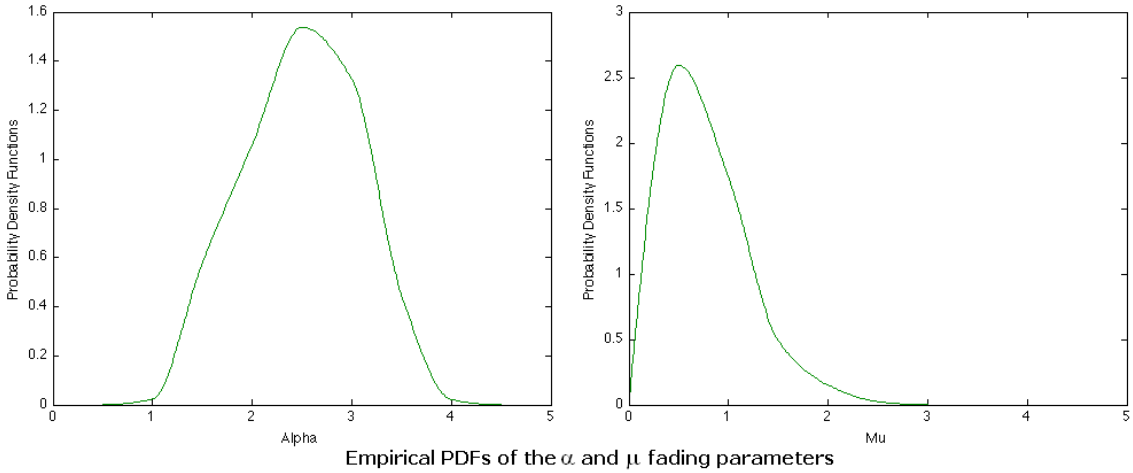

Fig. 4.30: PDF taken at Rua Cora Carolina Point 2

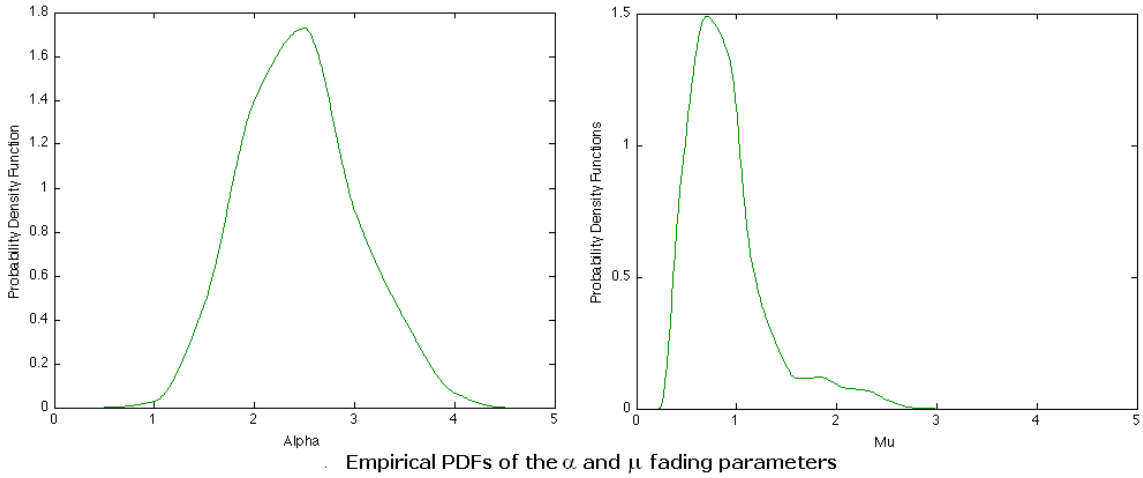

Fig. 4.31: PDF taken at Rua Cora Carolina Point 3

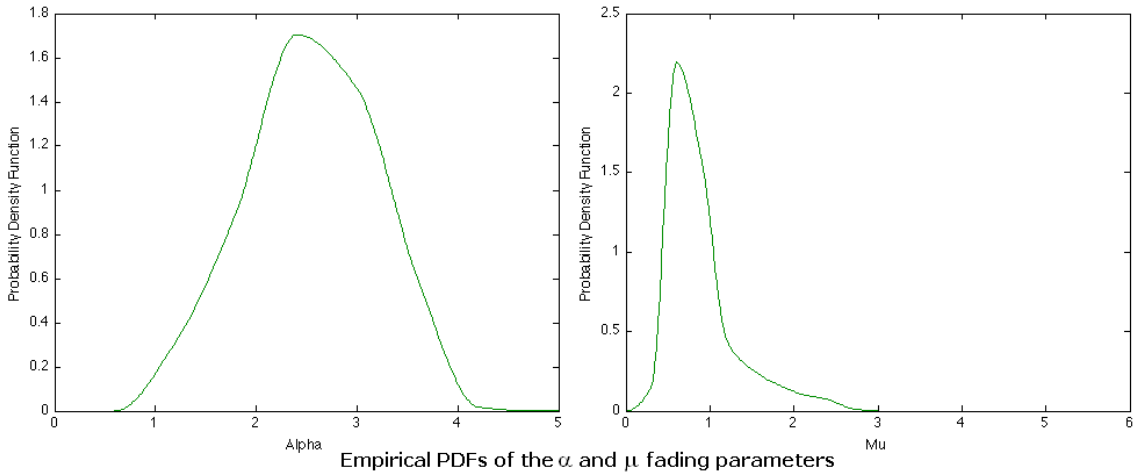

Fig. 4.32: PDF taken at Rua Cora Carolina Point 4

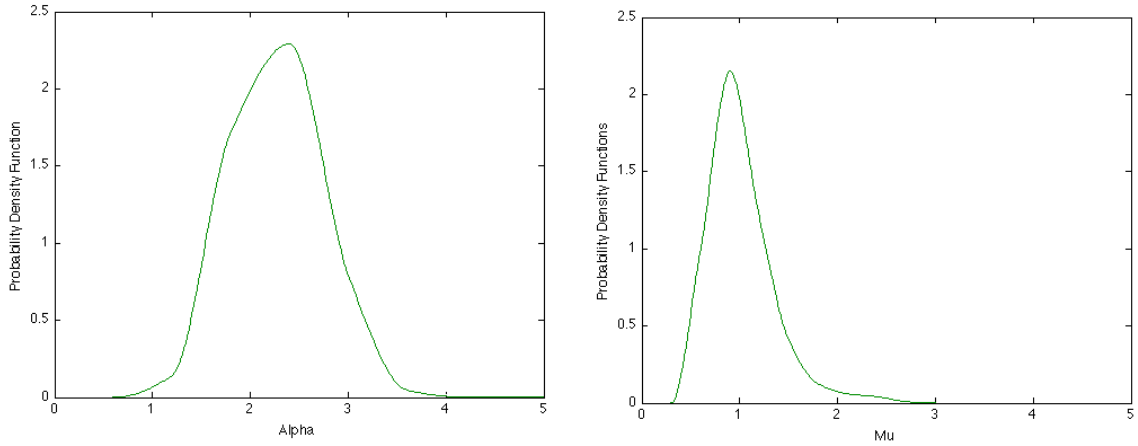

Fig. 4.33: PDF taken at Instituto de Economia Point 1

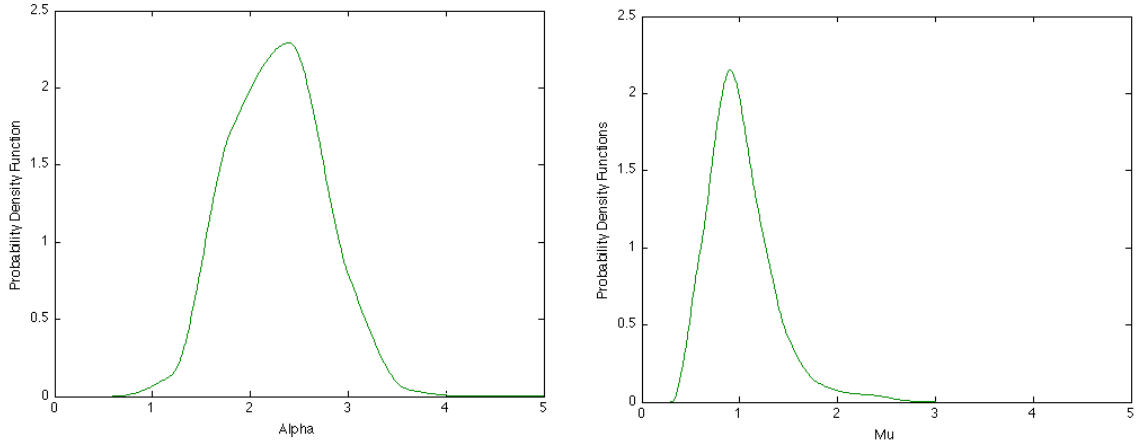

Fig. 4.34: PDF taken at Instituto de Economia Point 2

4.2.4 Magnitude Variations of the α and μ Fading Parameters

Figures 4.35 to 4.59 show sample plots of the magnitude variations of the α and μ fading parameters with distance. It can be seen that when α increases μ decreases, for a given displacement of the mobile receiver, and vice-versa. The physical phenomenon involved concern the following. When the magnitude of the nonlinearities of the propagation medium increases, the magnitude of the multi-path clustering decreases, possibly in an attempt to keep the variance of the power approximately constant meaning that the process is stationary. It must be said that the peak values (highest values assumed by α and correspondingly lowest values assumed by μ) occur when the dominant component appear in the propagation path. Conversely, the lowest values for α (and correspondingly highest values for μ)

occur when the dominant component is weak and there is a prevalence of multi-path clusters. These interesting behaviors involving the two fading parameters, as predicted by its theoretical model is now confirmed in practice.

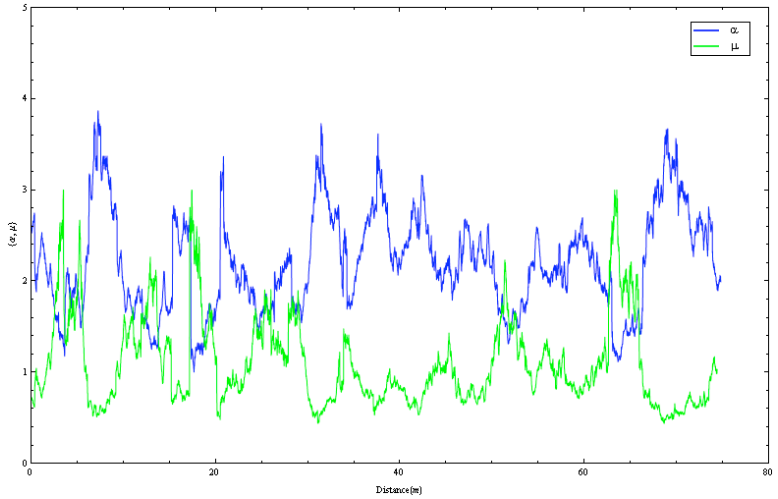

Fig. 4.35: Magnitude variations at Rua Luverci Pereira point 1

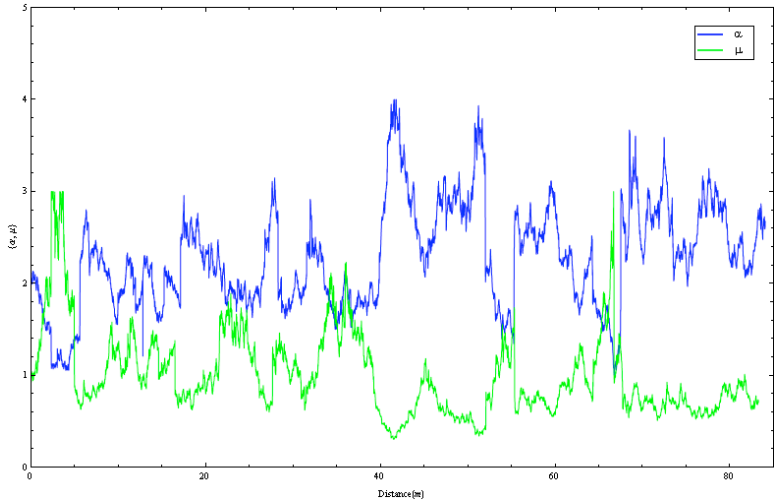

Fig. 4.36: Magnitude variations at Rua Luverci Pereira point 2

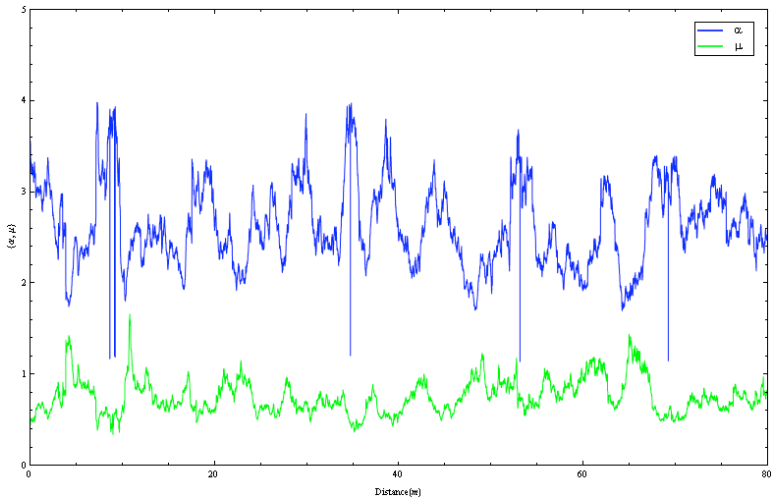

Fig. 4.37: Magnitude variations at Rua Luverci Pereira point 3

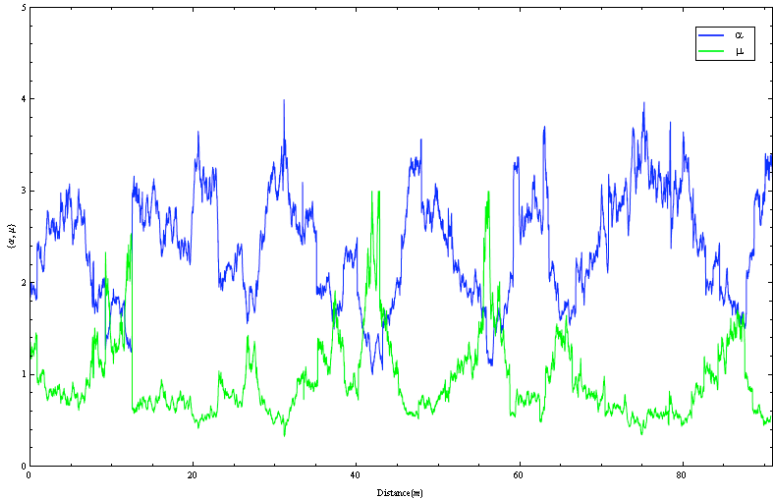

Fig. 4.38: Magnitude Variation at Rua Shegio Mori point 1

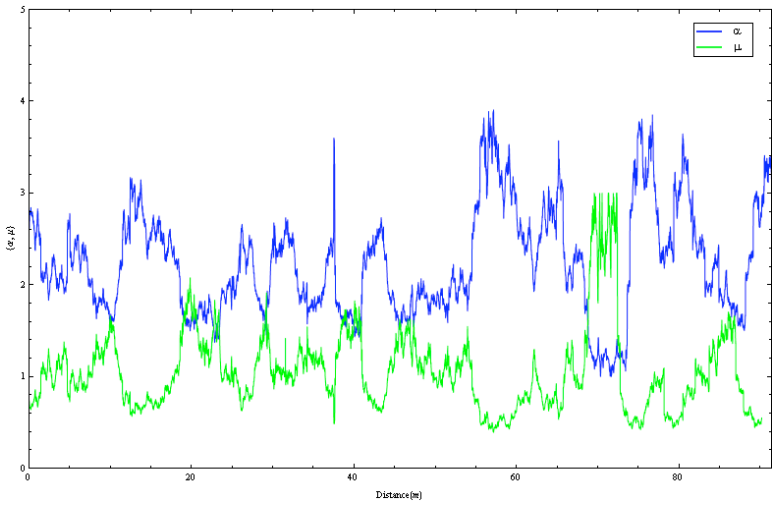

Fig. 4.39: Magnitude Variation at Rua Shegio Mori point 2

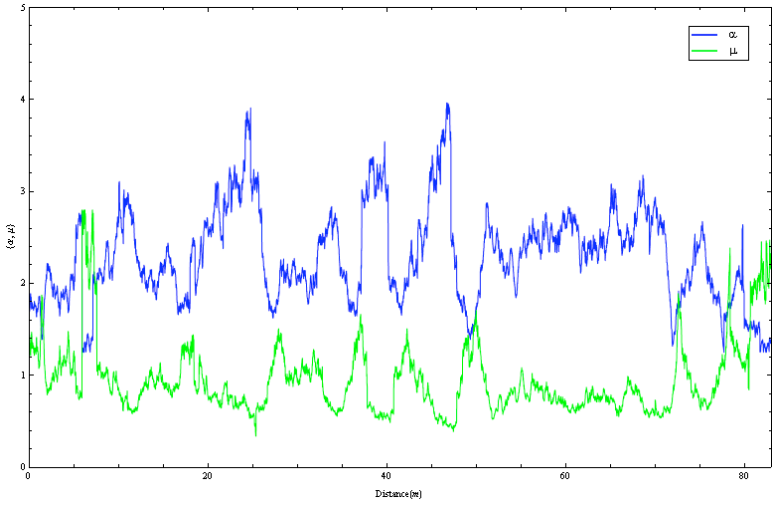

Fig. 4.40: Magnitude Variation at Rua Antonio Augusto point 1

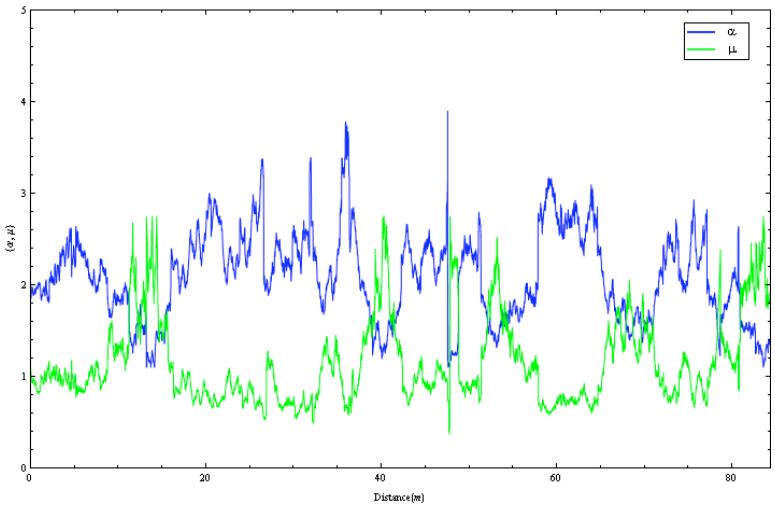

Fig. 4.41: Magnitude Variation at Rua Antonio Augusto point 2

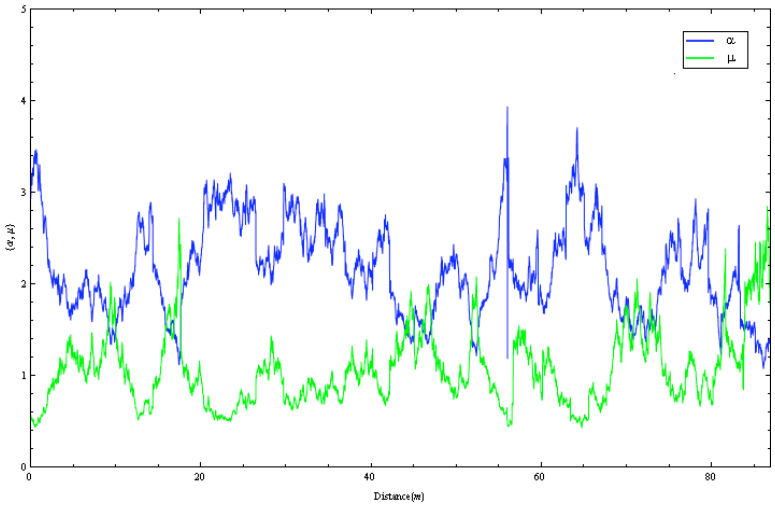

Fig. 4.42: Magnitude Variation at Rua Antonio Augusto point 3

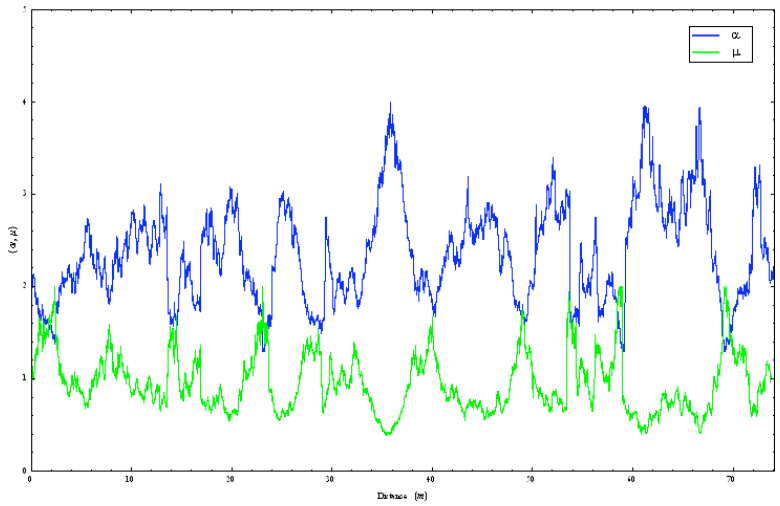

Fig. 4.43: Magnitude Variation at Av Prof Atilio Martins towards Downtown Point 1

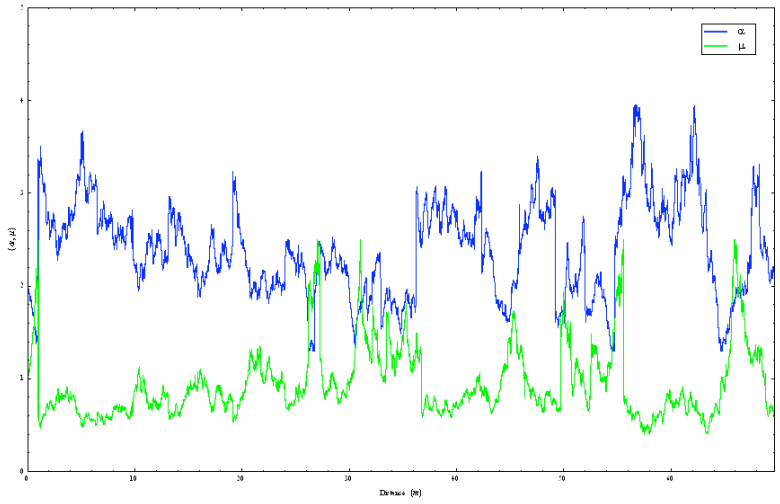

Fig. 4.44: Magnitude Variation at Av Prof Atilio Martins towards Downtown Point 2

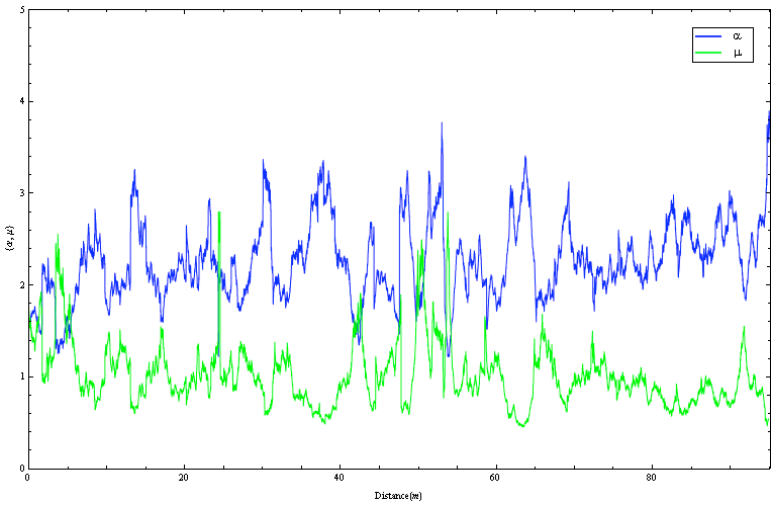

Fig. 4.45: Magnitude Variation at Instituto de Economia Point 1

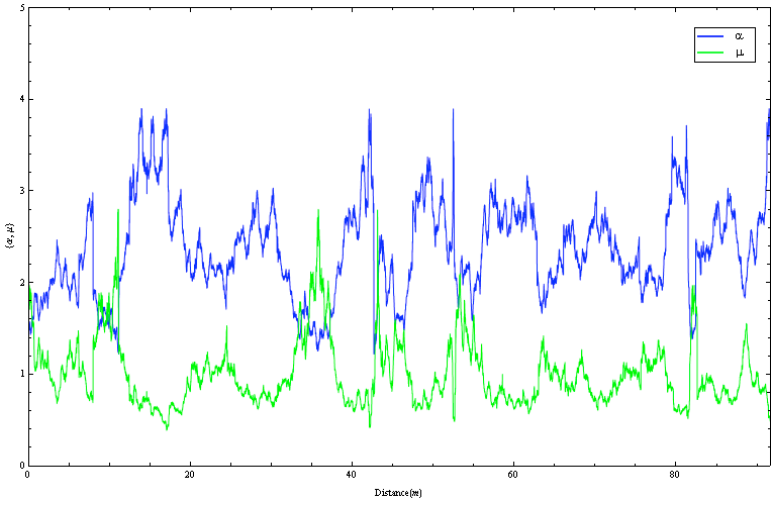

Fig. 4.46: Magnitude Variation at Instituto de Economia Point 2

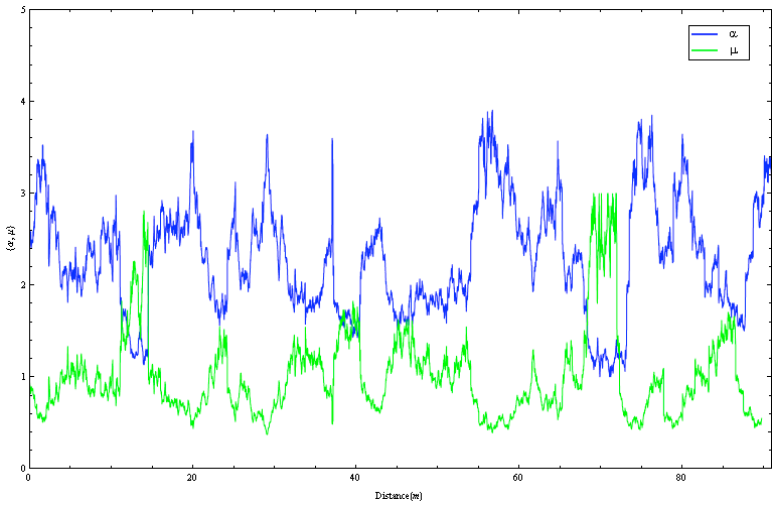

Fig. 4.47: Magnitude Variation at Av Prof Atilio Martins towards Unicamp point 1

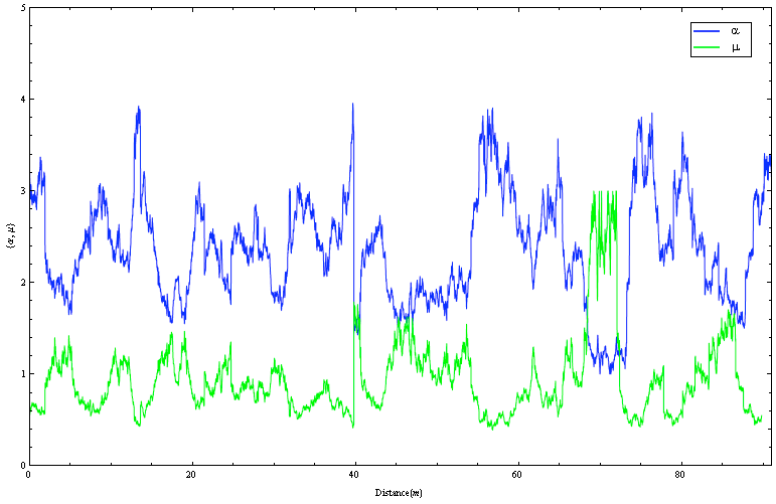

Fig. 4.48: Magnitude Variation at Av Prof Atilio Martins towards Unicamp point 2

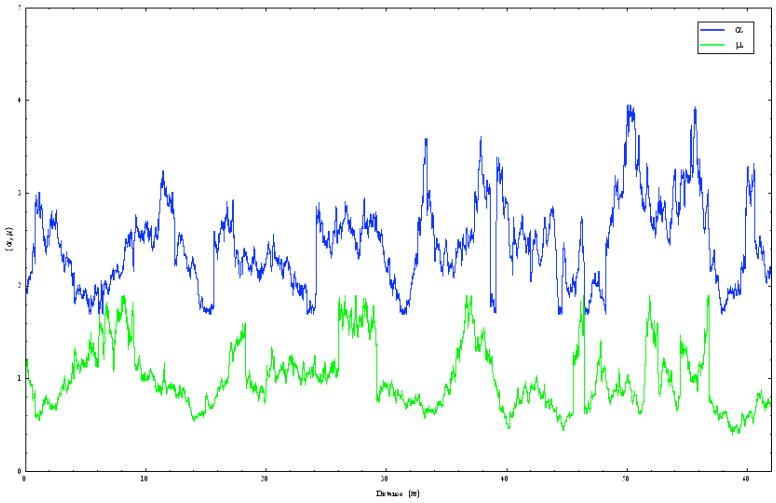

Fig. 4.50: Magnitude Variation at Av Prof Atilio Martins towards Unicamp point 4

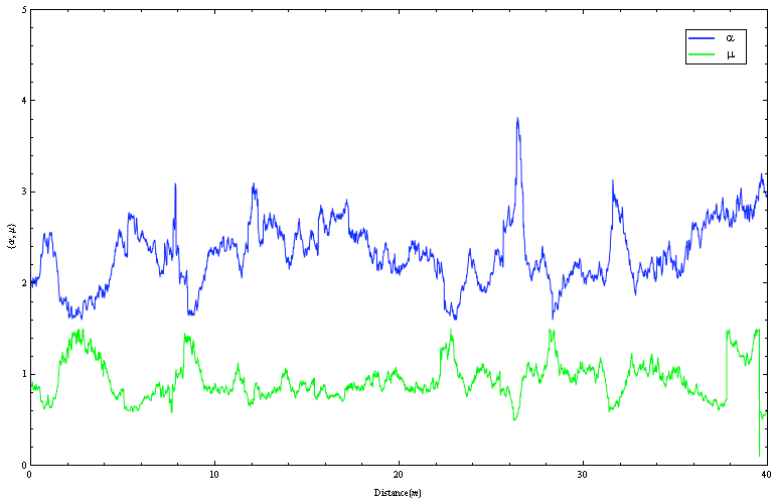

Fig. 4.49: Magnitude Variation at Av Prof Atilio Martins towards Unicamp point 3

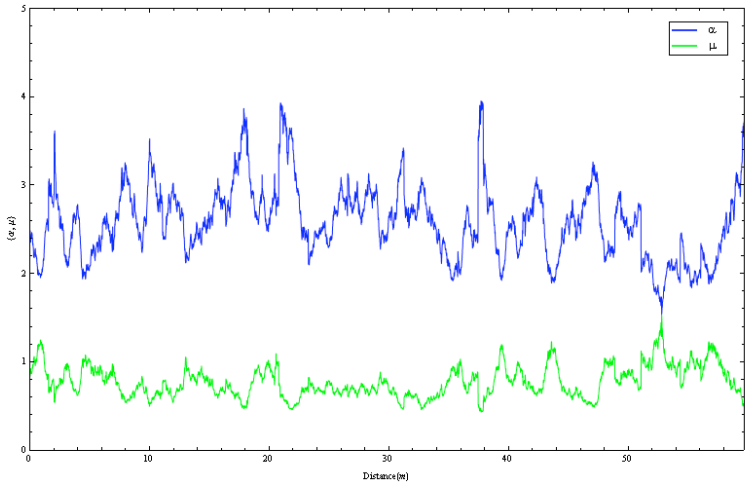

Fig. 4.51: Magnitude Variation at Rua Cora Carolina Point 1

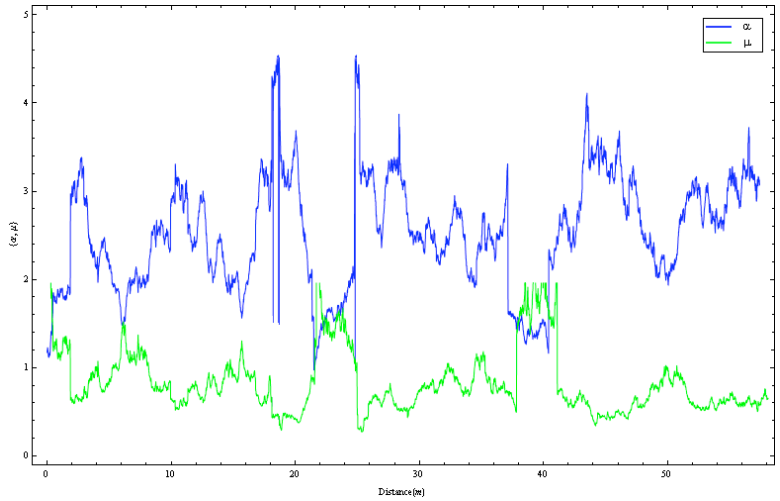

Fig. 4.52: Magnitude Variation at Rua Cora Carolina Point 2

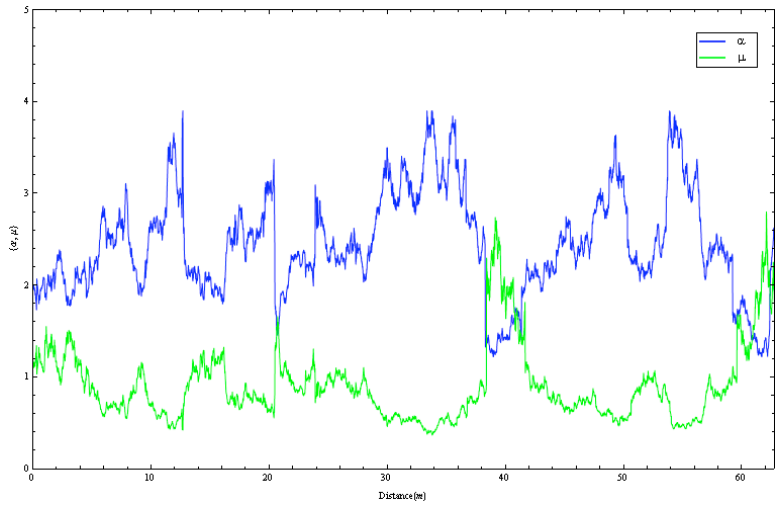

Fig. 4.53: Magnitude Variation at Rua Cora Carolina Point 3

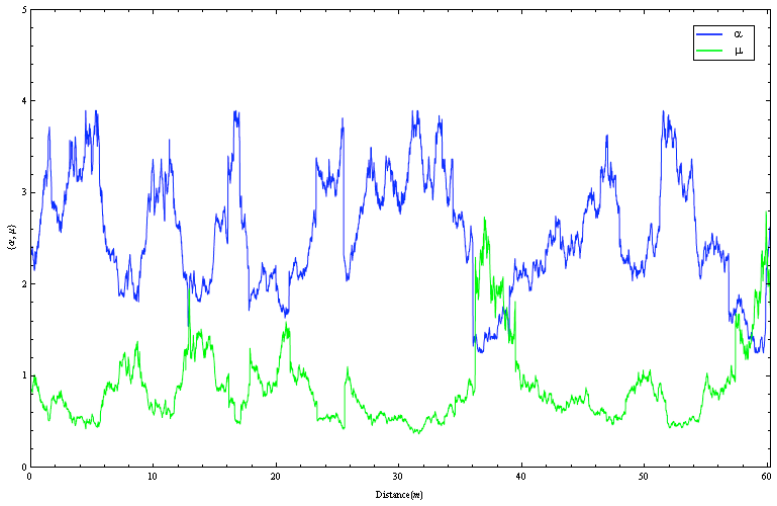

Fig. 4.54: Magnitude Variation at Rua Cora Carolina Point 4

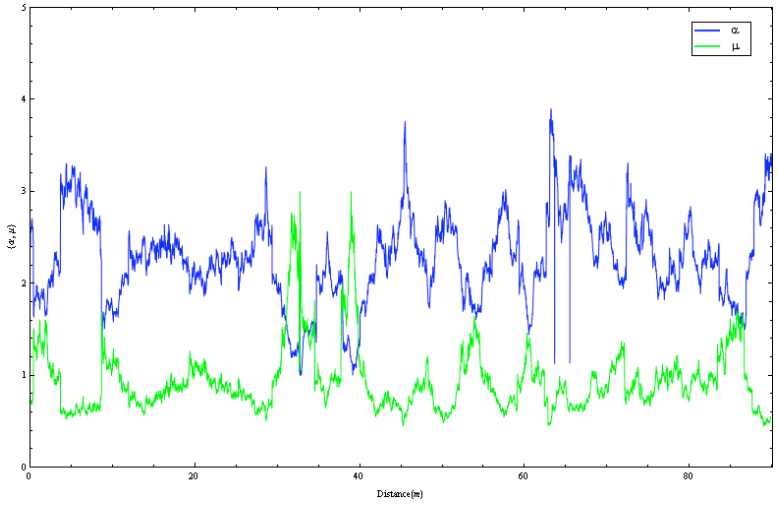

Fig. 4.55: Magnitude Variation at Rua Ruberlei point 1

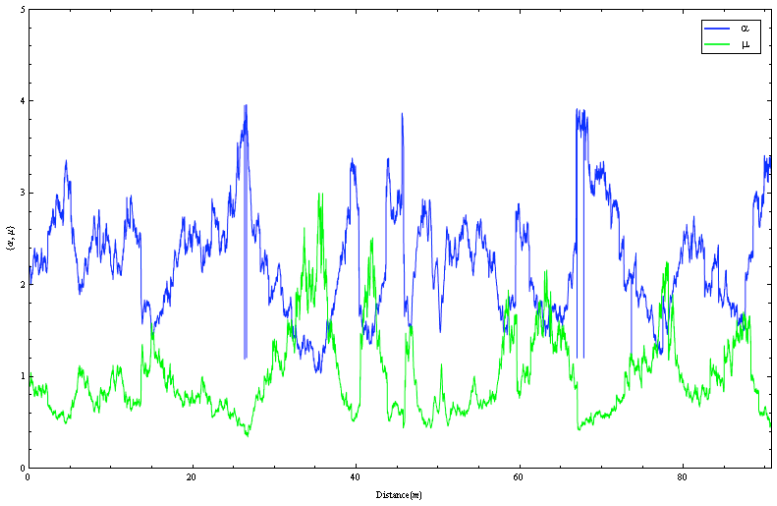

Fig. 4.56: Magnitude Variation at Rua Ruberlei point 2

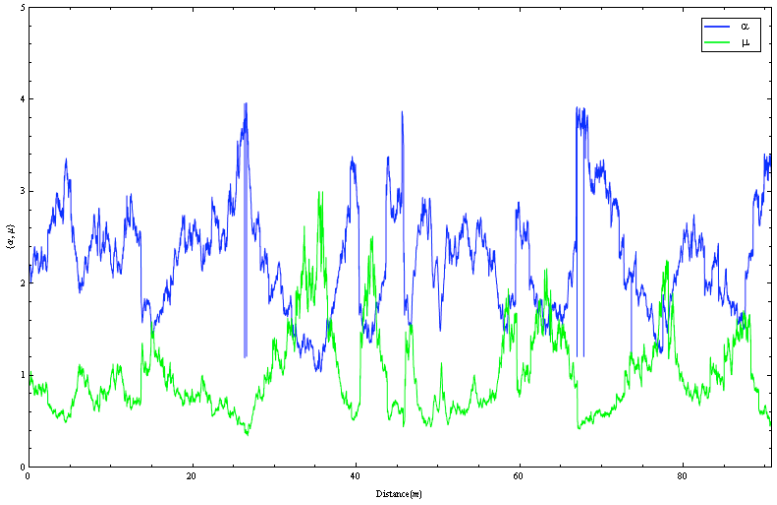

Fig. 4.57: Magnitude Variation at Rua Ruberlei point 3

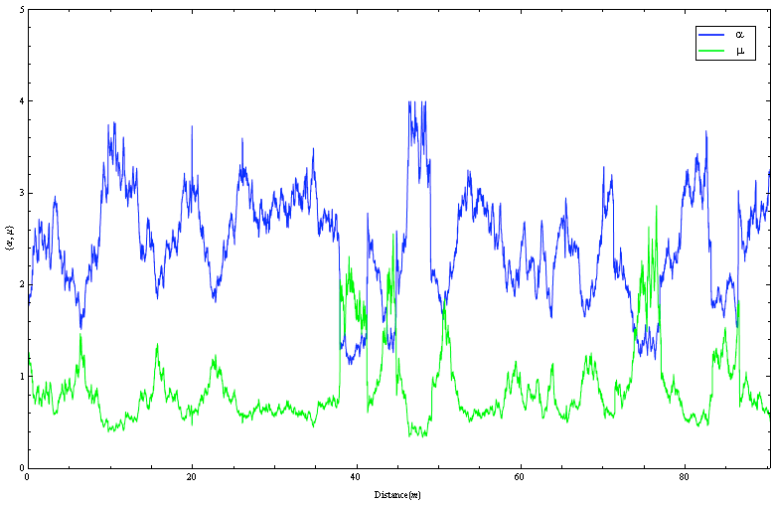

Fig. 4.58: Magnitude Variation at Parça Sergio Buarque Holanda point 1

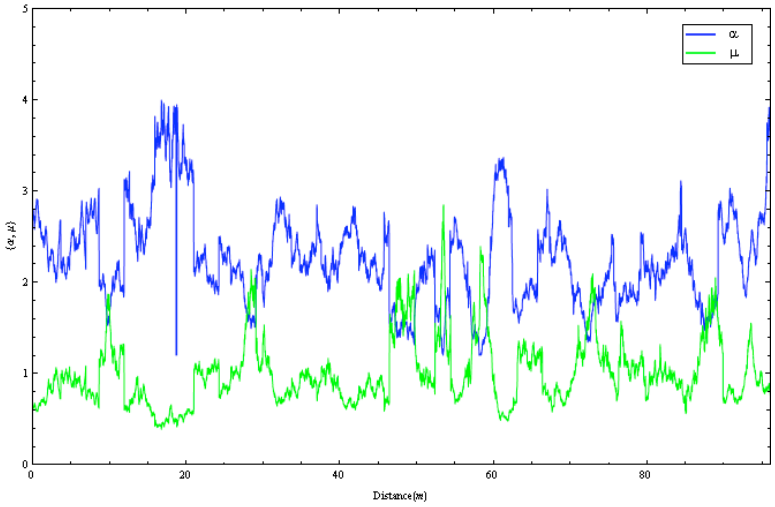

Fig. 4.59: Magnitude Variation at Parça Sergio Buarque Holanda point 2

4.2.5 Auto-correlation Functions(ACF)

Figures 4.61 to 4.68 depict the sample plots of the autocorrelation functions of the α and μ fading parameters in outdoor environments. Interestingly, we can observe how the α and μ curves tend to keep track of the changes in the concavity of each other with slight shifts. In most of the measured cases, the autocorrelation curves of α is found above the curves of μ.

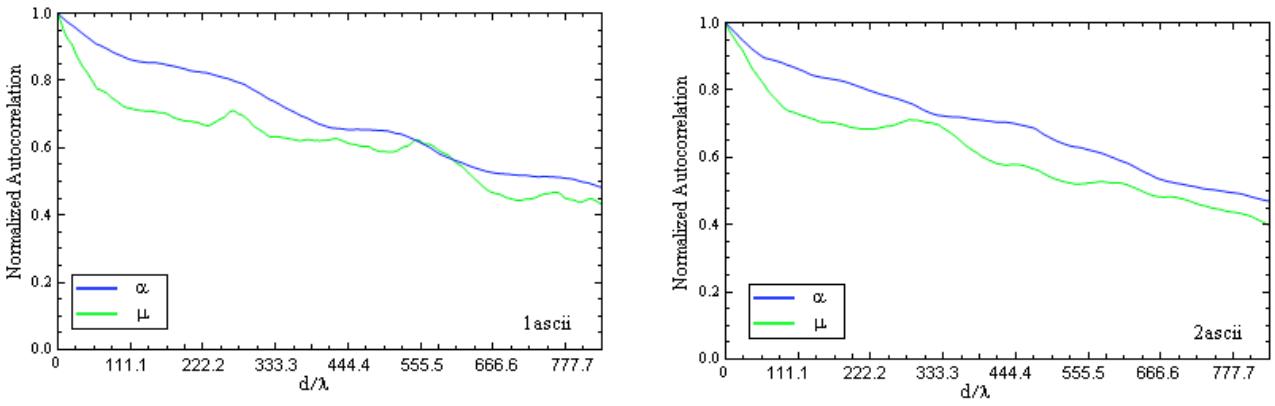

Fig. 4.60: ACFs at Rua Shegio Mori at points 1 and 2

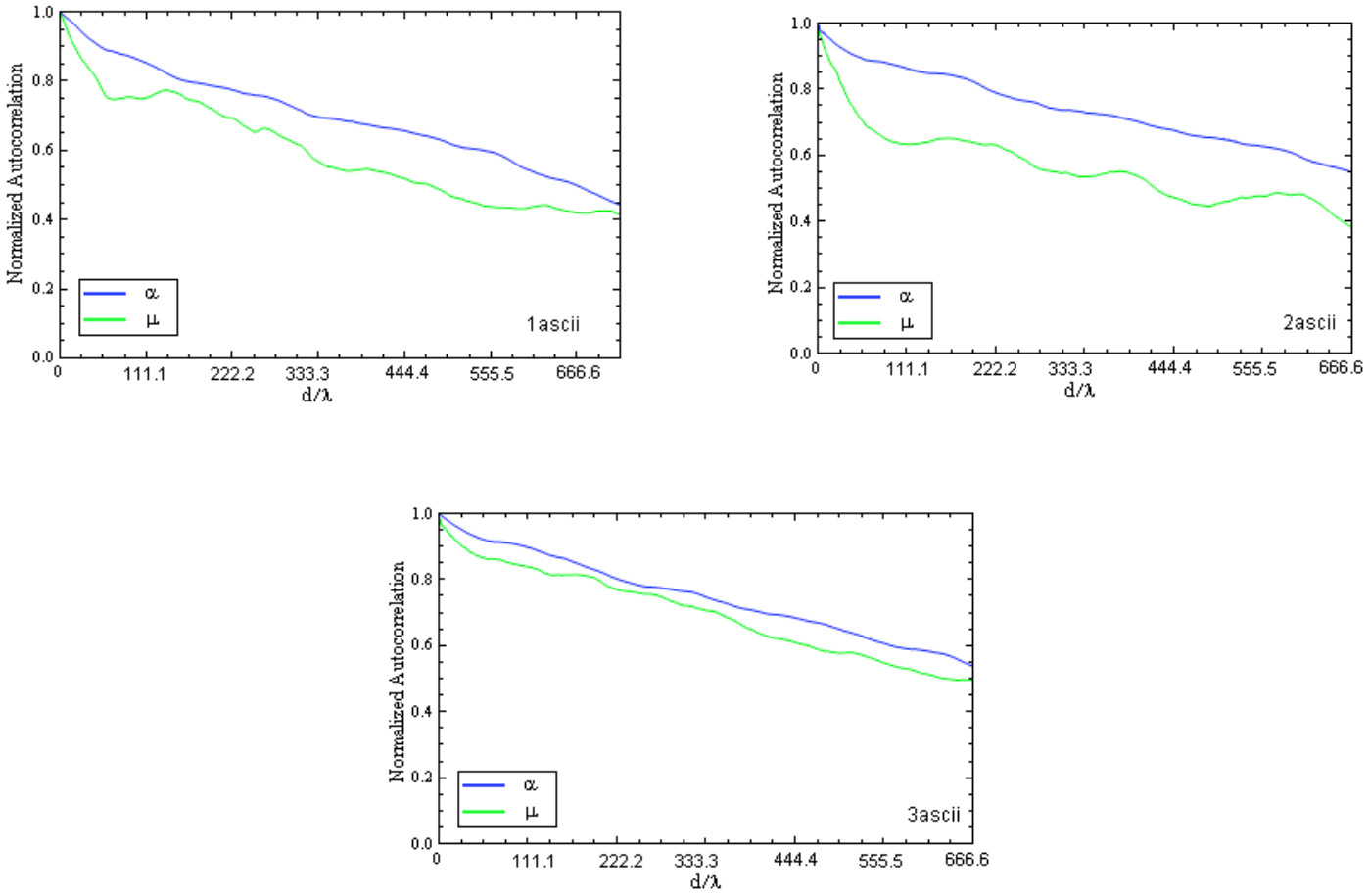

Fig. 4.61: ACFs at Rua Luverci Pereira at point 1,2 and 3

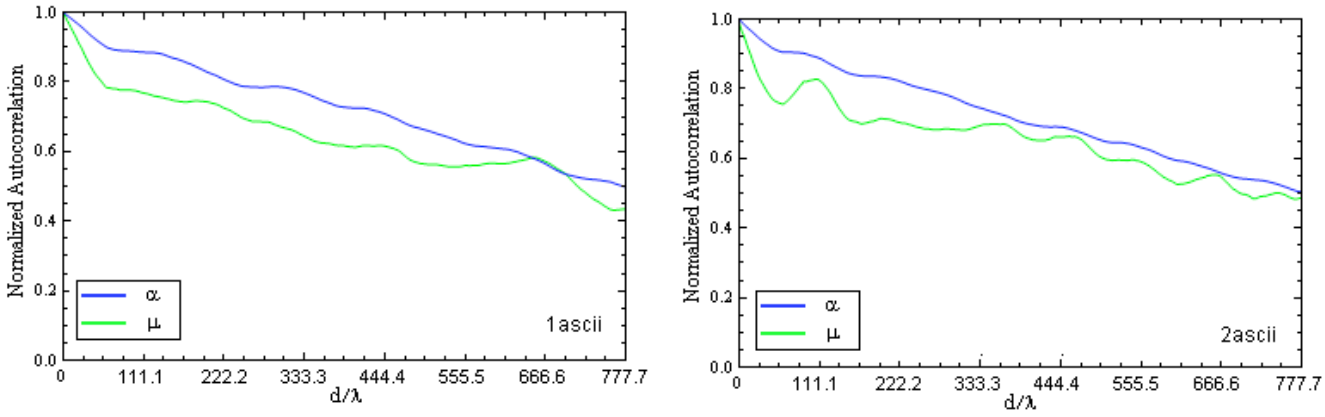

Fig. 4.68: ACFs at Rua S B Holanda side at points 1 and 2

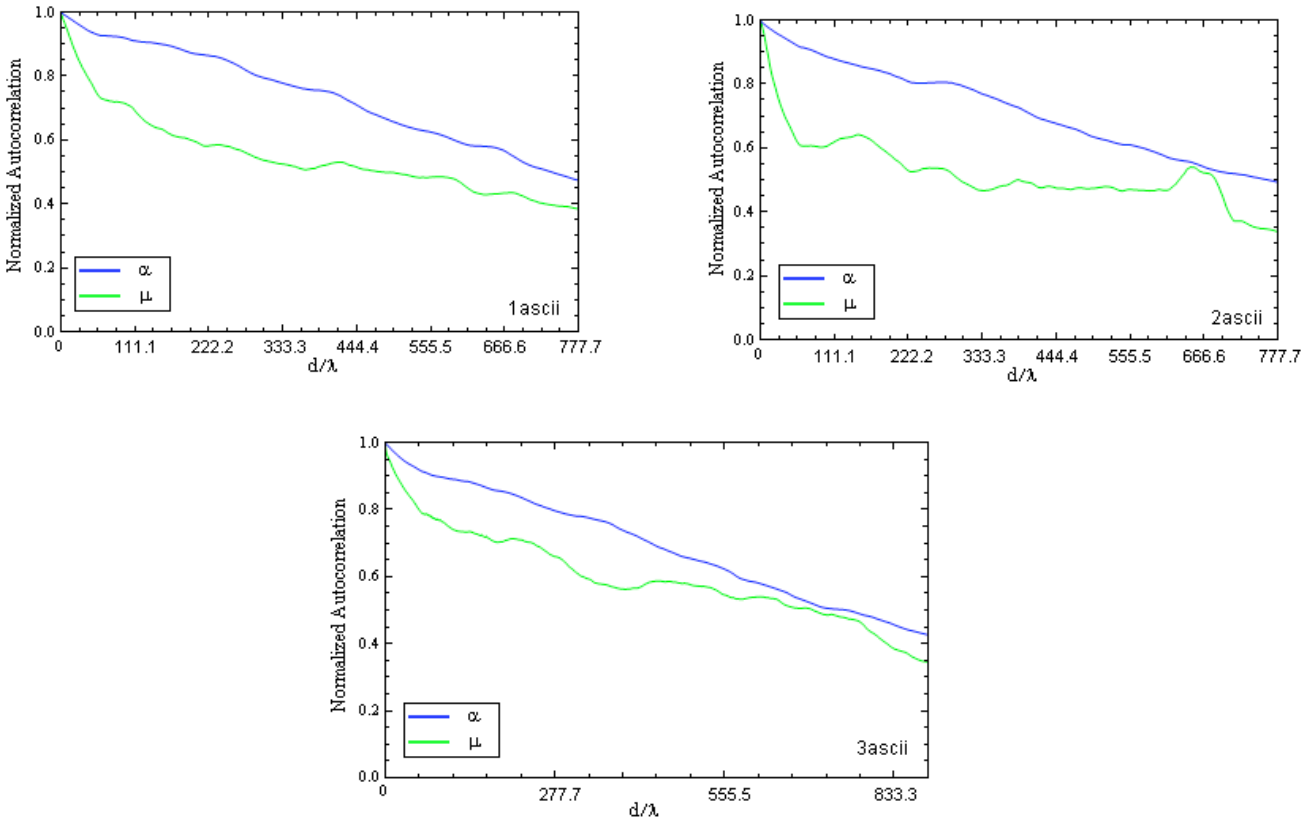

Fig. 4.62: ACFs at Rua Antonio Augusto at points 1, 2 and 3

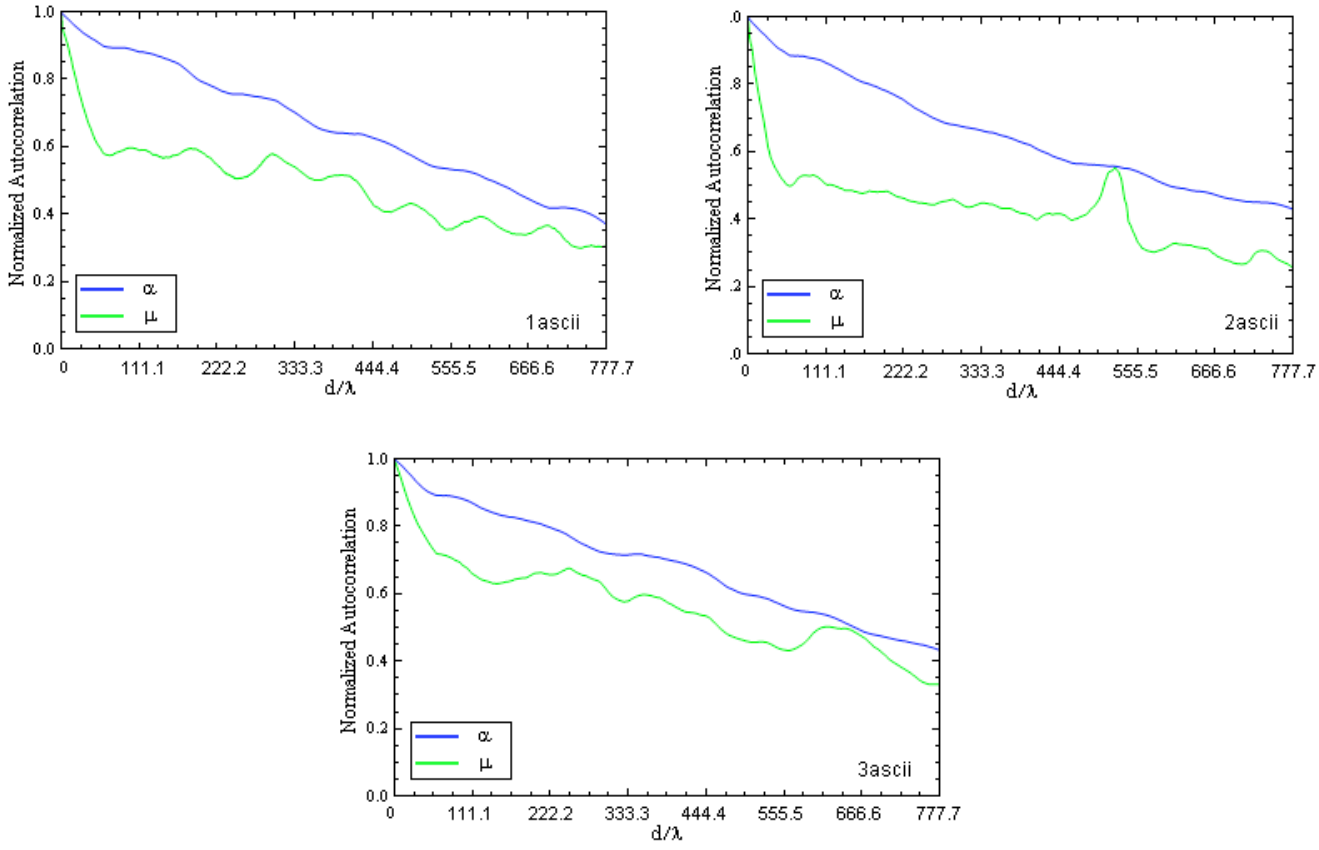

Fig. 4.63: ACFs at Avenida Atilio Martins downtown side at points 1, 2 and 3

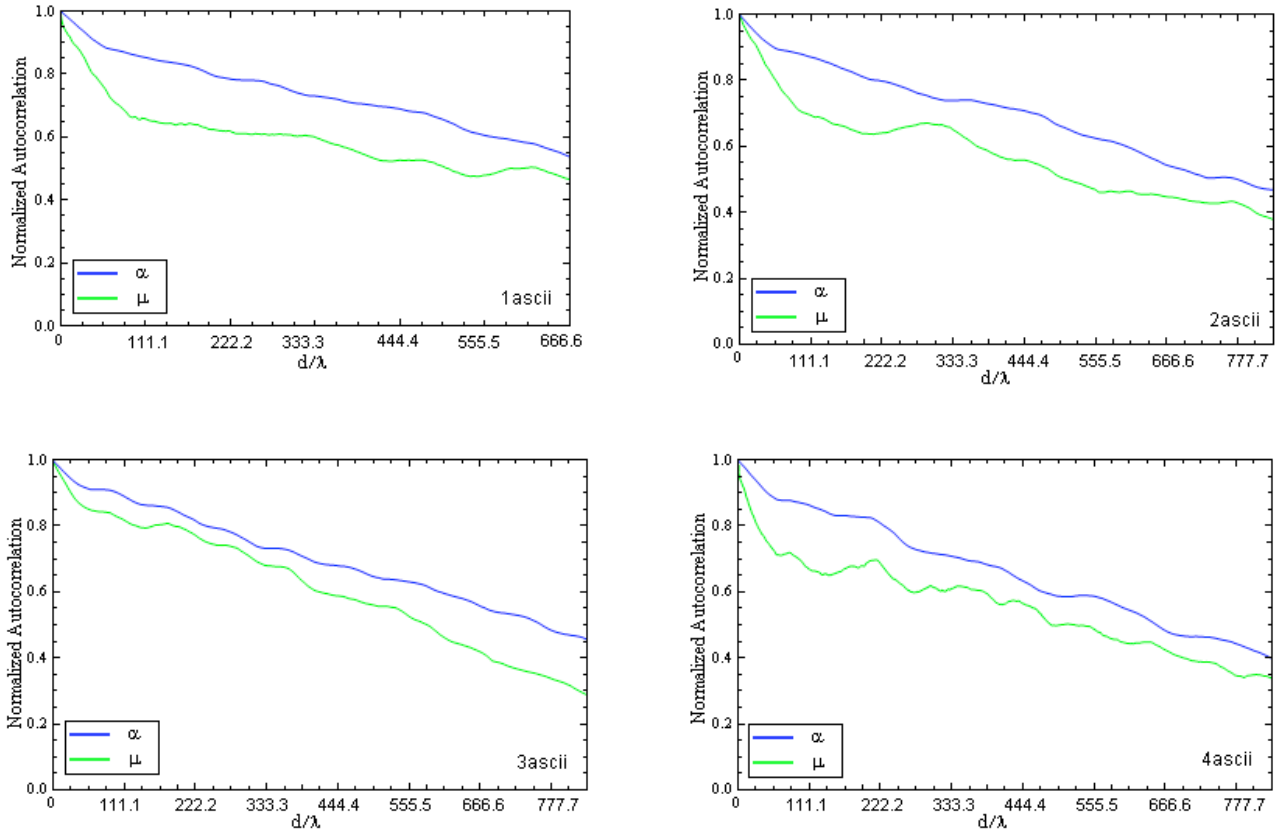

Fig. 4.64: ACFs at Avenida Atilio Martins Unicamp side at points 1, 2, 3 and 4

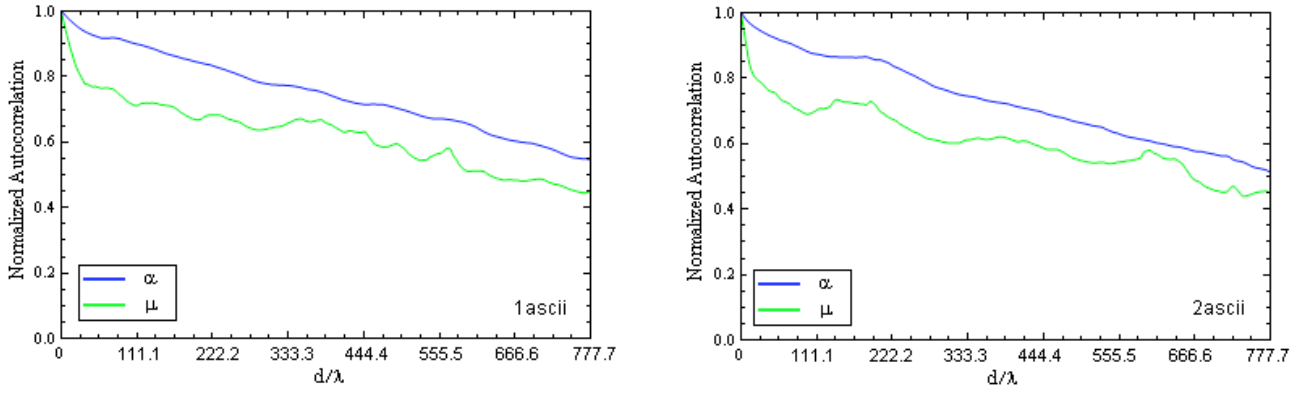

Fig. 4.65: ACFs at Instituto de Economia side at points 1 and 2

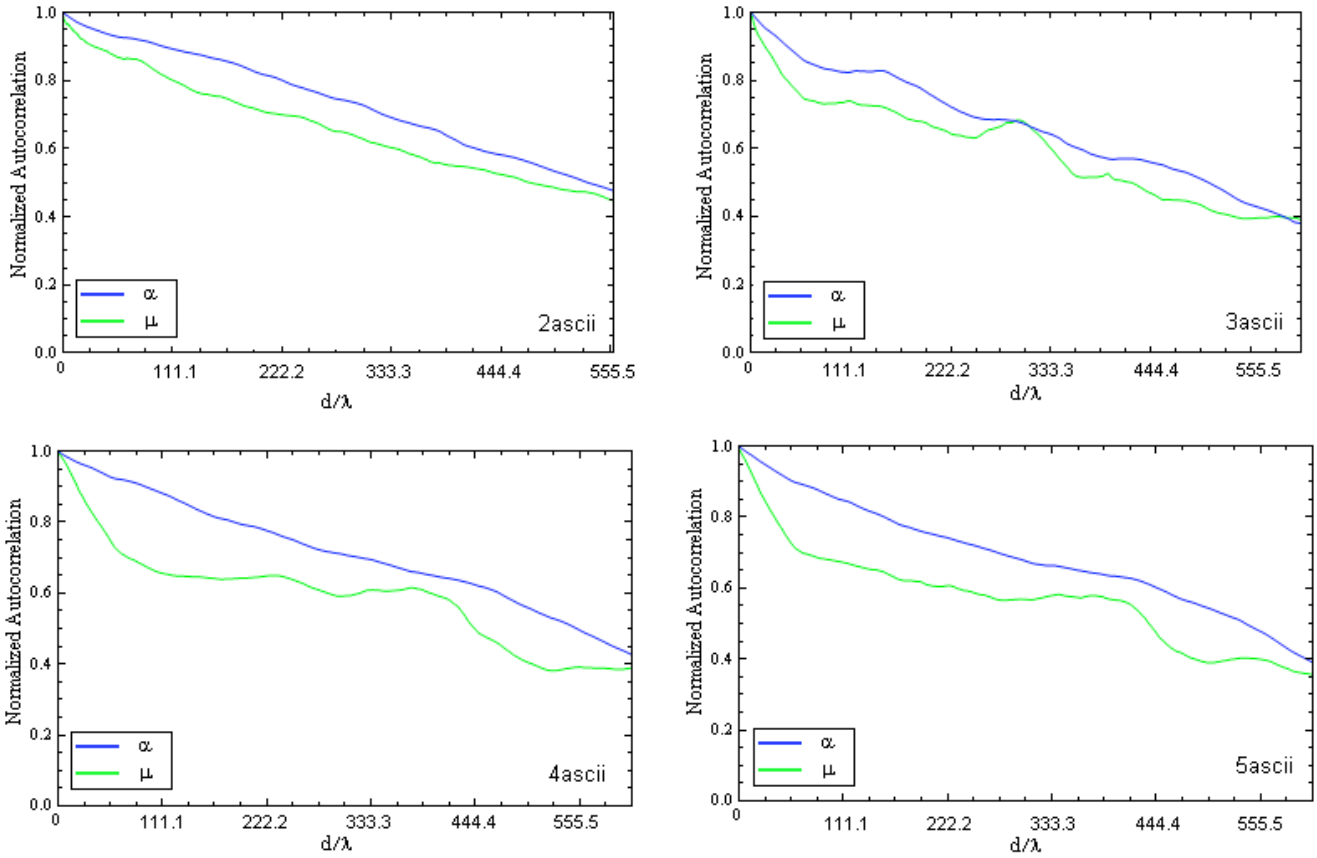

Fig. 4.66: ACFs at Rua Cora Carolina side at points 1, 2, 3 and 4

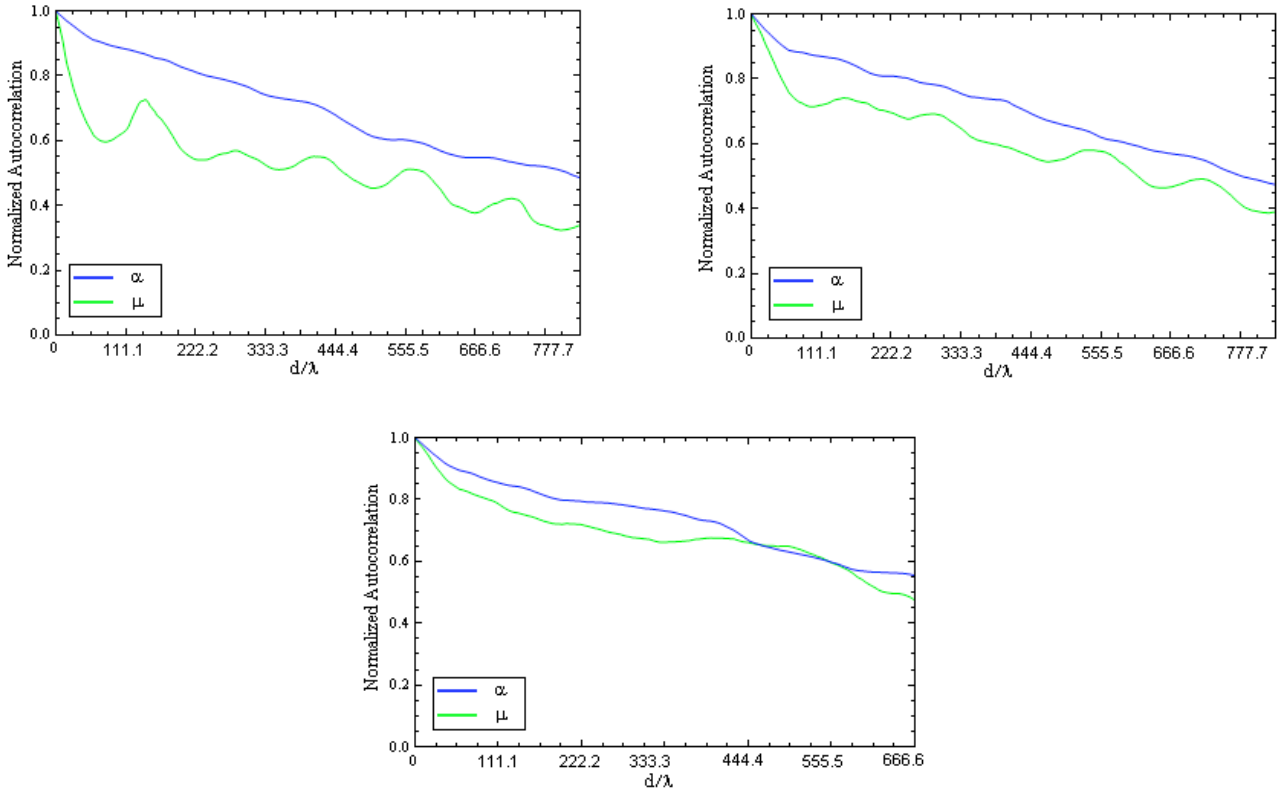

Fig. 4.67: ACFs at Rua Ruberlei side at points 1,2 and 3

4.3 Conclusion

In this chapter we presented the methodology and techniques used in our field trials for acquiring the data using the mobile reception unit. The empirical probability density functions and the auto-correlation functions of the α and μ fading parameters were also presented. The mean, median and standard deviation values of the fading parameters were reported. Furthermore, the ranges of possible practical values of the α and μ fading parameter were estimated from the empirical data, and the instantaneous variations of their magnitudes were evaluated considering the displacement of the mobile receiver in all kinds of outdoor environments.

Chapter 5

Conclusion

5.1 Conclusion

In this thesis, the major elements that contribute to the multi-path fading were characterized using the α-μ Distribution. The α-μ Distribution was revisited and a brief description on the α-μ fading model was presented.

Although the α-μ distribution has one parameter more than that of Nakagami-m and Weibull Distributions, no additional difficulty is posed by the increase in the number of parameters. Also, the flexibility of the α-μ Distribution conveys is outstanding and renders it suited to better adjust to field data. Using this fading model, we were able to develop first and higher order statistics of the α-μ Distribution.

Field measurements were successfully conducted using a field measurement vehicle as described in chapter 3. Also, transmission system was setup with a stationary transmitter and a mobile reception vehicle acting as the receiver. All the data were carefully collected and analyzed to obtain the first and higher order statistics of the α-μ Distribution.

More specifically, the empirical probability density functions and autocorrelation functions of the α-μ fading parameter were obtained. In addition, the possible practical ranges of values for the α and μ fading parameter were estimated from the empirical data, and variations of their instantaneous magnitudes were evaluated, considering the displacement of the mobile receiver in outdoor environments. These results provide important information about the practical utility of the α-μ fading model in mobile communication systems. The schemes discussed have shown that the knowledge of the α and μ fading parameters helps us to design a better communications system with better performance. It is our hope that this thesis contributes to the ever growing field of Wireless Communications helping to better understand the planning and designing of such wireless communications systems with utmost performance.

5.2 Future work

Radio mobile engineering is a fast evolving area in which a vast amount of research is going on and each day a new technology is being developed as the old become obsolete. The future of this work could be a continuation of the same topic which may focus on characterization of the κ-μ and η-μ distributions for their fading parameters. A similar work can be carried out using the α-μ distribution in much diverse kinds of environments for example: densely forested areas, highly populated metropolitan city areas and etc. Future field measurements could also be carried out using multiple receivers and transmitters, with other frequencies like 2.4 GHz, 3.5GHz and etc. The obtained data can be used in order to model a more realistic wireless system, for which the fading parameters vary along the radio path.

5.3 Conclusão

5.3.1 Conclusão

Nesta tese, os elementos principais que contribuem para o *multi-path fading* foram caracterizados usando a distribuição α-μ . A distribuição α-μ foi revisada e uma descrição breve do modelo do desvanecimento α-μ foi apresentada. Embora a distribuição α-μ tenha um parâmetro a mais do que as distribuições de Nakagami-m e Weibull, nenhuma dificuldade adicional é inserida pelo aumento no número de parâmetros. Também, a flexibilidade na transmissão da distribuição α-μ é notável e a torna adequada para um melhor ajuste aos dados de campo. Usando o modelo fading foi possível desenvolver as estatísticas de primeira ordem e ordem superior da distribuição α-μ.

Medidas de campo foram conduzidas com sucesso usando-se um veículo de medida de campo, como descrito no capítulo 3. Também, o sistema de transmissão foi instalado com um transmissor estacionário e um veículo de recepção móvel que atua como o receptor. Os dados foram cuidadosamente coletados e analisados para se obter as estatísticas de primeira ordem e ordem superior da distribuição α-μ.

Mais especificamente, as funções empíricas de densidade de probabilidade e funções de autocorrelação para os parâmetros do α-μ foram obtidas. Adicionalmente, os intervalos práticos possíveis de valores dos parâmetros para desvanecimento tipo α e μ foram estimadas de dados empíricos e variações dessas magnitudes instantâneas foram avaliadas, considerando o deslocamento do receptor móvel em ambientes abertos. Esses resultados fornecem importantes informações sobre a utilidade prática do modelo α-μ em sistemas de comunicação móveis. Os esquemas discutidos mostram que o conhecimento dos parâmetros de desvanecimento α-μ nos ajudam a projetar um melhor sistema de comunicação com melhor performance. Esperamos que esta tese contribua para o crescente campo das telecomunicações sem fio e ajude no melhor entendimento do planejamento e projeto de sistemas de comunicação sem fio semelhantes e com o máximo desempenho.

5.3.2 Trabalhos Futuros

A engenharia de rádio móvel é uma área que atualmente encontra-se em franca evolução em decorrência da grande quantidade de pesquisa que está sendo realizada. A cada dia, novas tecnologias surgem e acabam por substituir as tecnologias anteriormente empregadas. O futuro deste trabalho pode ser a continuação do mesmo, porém focando-se na caracterização da distribuição κ-μ e distribuição η-μ para esses parâmetros do desvanecimento. Um trabalho similar pode ser realizado usando a distribuição α-μ nos mais diversos tipos de ambientes, como por exemplo: áreas densamente florestadas, áreas de cidades metropolitanas altamente populosas, etc. Medidas de campo futuras po-

dem também ser realizadas utilizando-se receptores e transmissores múltiplos, com frequências de ordem mais alta como 2.4 GHz, 3.5 GHz, etc. Os dados obtidos podem ser usado para modelar um sistema sem fio mais realista, para os quais os parâmetros variam fading ao longo do trajeto de rádio..

Bibliography

[1] Dr. Ing Erik Haas. Aeronautical Channel Modelling. *Personal Website Online*.

[2] Andrea Goldsmith. *Wireless communications*. Cambridge University Press, 2005.

[3] W. C. Jakes. *Microwave Mobile Communications*. Wiley, 1974.

[4] Michel Daoud Yacoub. *Foundations of mobile radio engineering*. CRC Press, 1993.

[5] W. C. Lee. *Mobile Communications Engineering*. McGraw Hill, 1998.

[6] COST Action 231 Digital Mobile Radio Towards Future Generation Systems. *Final Report*, 1999.

[7] H. H. Xia L. R. Maciel, H. L. Bertoni. Unified approach to predicion of propogation over buildings for all ranges of base station antenna height. *IEEE Transaction on Vehicular Technology*, 43(1):35–41, February 1993.

[8] G. L. Turin. Introduction to Spread-Spectrum Antimultipath Techniques and Their Application to Urban Digital Radio. pages 328–353, March 1980.

[9] L.Rayleigh. On the resultant of a large number of vibrations of the same pitch and of arbitrary phase. August 1880.

[10] S.O.Rice. Statistical properties of a sine wave plus random noise. pages 46–156, January 1948.

[11] R.S.Hoyt. Probability functions for the modulus and angle of the normal complex variate. pages 318–359, April 1947.

[12] M. Nakagami. The m-Distribution - A General Formula of Intensity Distribution of Rapid Fading. *Statistical Methods in Radio Wave Propagation by W. C. Hoffman, Ed. Elmsford, NY: Pergamon*, 58:3–36, Oct. 1960.

[13] M. D. Yacoub. The κ-μ distribution: A general fading distribution. pages 1427–1431, October 2001.

[14] M. D. Yacoub. The η-μ distribution: A general fading distribution. pages 872–877, September 2000.

[15] M. D. Yacoub. The α-μ distribution: A general fading distribution. September 2002.

[16] E. W. Stacy. A generalization of the Gamma distribution. *Annal. Math. Stat*, 33(3):1187–1192, Sept 1962.

[17] U. S. Dias, M. D. Yacoub. On The α-μ Autocorrelation and Power Spectrum Functions: Field Trials and Validation. November-December 2009.

[18] Qiong Wu, David W. Matolak, and Indranil Sen. $5-GHz-Band$ Vehicle to Vehicle Channels: Models for Multiple Values of Channel Bandwidth. pages 2620–2625, June 2010.

[19] A. Michalopoulou1, T. Zervos, K. Peppas, F. Lazarakis, A. A. Alexandridis, K. Dangakis, D. I. Kaklamanim. On-body Diversity Channels at 2.45 GHz: Measurements and Statistical Analysis. pages 2982–2986, 2011.

[20] Petros Karadimas, Efstathios D. Vagenas, and Stavros A. Kotsopoulos. On the Scatterers' Mobility and Second Order Statistics of Narrowband Fixed Outdoor Wireless Channels. pages 2119–2124, June 2010.

[21] Poh Kit Chong, Seong-Eun Yoo, Seong Hoon Kim, and Daeyoung Kim. Wind-Blown Foliage and Human-Induced Fading in Ground-Surface Narrowband Communications at 400MHz. pages 1326–1336, May 2011.

[22] W. R. Braun and U. Dersch. A physical mobile radio channel model. *IEEE Trans. Veh. Technol.*, 40(2):472–482, May 1991.

[23] M.D.Yacoub. The α-μ Distribution: A physical Fading Model for the Stacy Distribution. *IEEE Transactions on Veh. Technol.*, 56:27–34, Jan 2007.

[24] H. B. Tercius, M. D. Yacoub, L. F. Crocomo, L. C. Kretly, F. C. Martins, and A. F. de Toledo. Eadmec - Equipamento de Aquisição de Dados Modular Espacialmente Controlado. September 2003.

Appendix A

Technical Specifications

This appendix provides the technical specifications of the components used in assembling the transmitter and the data acquisition equipment. The equipment is designed to operate in the frequency of operation of 5500MHz

Technical specifications of the components used in assembling the transmitting antenna;

- **Transmitting Antenna**: HUBER+SUHNER, Sucotest SMA M SMA M 72 in DC to 18 GHz.
- **Signal Generator**: Agilent, modelo e8257d.
- **Power Amplifier**: Hughes TWT, modelo 1177H06F000.
- **Transmission cable**: Andrew FSJ4-50B. Approximately 6,2 m between the TX antenna and the power amplifier and another of 1.20 m between the generator and the amplifier.

Technical specifications for the mobile reception unit follows;

- **Sprocket**: Made of aluminum plate of 1.2mm, with 57 teeth. This wheel is coupled to a fifth wheel that is attached to data acquisition equipment via a mechanical arm. This arm allows the movement of the fifth wheel assembly/wheel in the vertical direction.
- **Circuit sampler**: Once described in Section 3.2.1.
- **Receiving Antenna**: Kathrein, model 800 10249. Operating frequency range 806-6, 000MHz,gain of 2dBi.
- **Attenuator**: Agilent, model 8496 A. Manual attenuator with frequencies in the range of 0 - 4GHz with variable attenuation 0 - 110dB in steps of 10dB.

- **Amplifier(low noise amplifier)**: Mini-circuits, model-Kathrein, model $8449b$, 30dB gain, Frequency of operation $1,700$-2400MHz. Amplification 40dB and power in the range of 12 - 16VDC.
- **Spectrum Analyzer**: HP, model E 8593, with operating frequency of 0 - 22GHz
- **Laptop**: Toshiba Satellite model 1800-S254. Pentium III GHz 1, 1 Gb of RAM, hard drive 20 Gb 14.1"TFT screen.
- **Drive**: SMS Brand, Manager III sinusoidal model. Maximum output power of 1300 VA, input voltage V 127, Output frequency Hz $60to \quad pm$ 1 %.
- **Cable**: Huber+Suhner Sucotest. Comprimento: A 72 inch cable between the reception antenn and amplifier e outher cable of 48 inches between the amplifier and the spectrum analyzer.
- **Battery**: Two batteries. AC Delco brand, model 011AO63D1, V 12, 63 Ah.

Appendix B

Post-processing programming codes

In this appendix we will see the programming codes used in *Mathematica 8* for post processing of the received data files.

```
(**Importing the file received from the Laptop for post processing of the collected datas**)

A=Import["C:/Documents and Settings/aravind/My
Documents/Downloads/files03/1/3ascii_RMS.txt","Table"];
B=Table[0,{i,1,Length[A]}];
For[i=1,i≤Length[A],i++,B[[i]]=A[[i,1]];]
final=Length[Transpose[A]];
c=Table[0,{i,1,Length[A]-2}];
For[i=2,i≤final,i++,c[[i]]=Part[A,All,i]]
Z=
Join[c[[2]],c[[3]],c[[4]],c[[5]],c[[6]],c[[7]],c[[8]],c[[9]],c[[10]],
c[[11]],c[[12]],c[[13]],c[[14]],c[[15]],c[[16]],c[[17]],c[[18]],c[[19
]]];



(**Using the Moving Average method**)

media=MovingAverage[Z,10800];
media2 = MovingAverage[Z^2,10800];
media4 = MovingAverage[Z^4,10800];



(**Finding out the alpha and mu parameters**)

For[ i=1, i≤Length[media], i++,
 R1=media[[i]]; R2=media2[[i]]; R4=media4[[i]];
 {α,μ}={α,μ}/.FindRoot[{R1^2/(R2-R1^2)-Gamma[μ+1/α]^2/(Gamma[μ]
Gamma[μ+2/α]-Gamma[μ+1/α]^2)==0,R2^2/(R4-R2^2)-
Gamma[μ+2/α]^2/(Gamma[μ] Gamma[μ+4/α]-
Gamma[μ+2/α]^2)==0},{α,1},{μ,1}];
 P1[i]={α,μ} ;
 ]

(** Saving the values as txt file for calculating the first-and second-order statistics**)

Save["0313ascii.txt",P1]
P1[1][[1]];
```